



**HAL**  
open science

## **Low-thrust Interplanetary Trajectories with Missed Thrust Events: a Numerical Approach**

Jean-Philippe Chancelier, Pierre Carpentier, Guy Cohen, Thierry Dargent, Richard Epenoy

► **To cite this version:**

Jean-Philippe Chancelier, Pierre Carpentier, Guy Cohen, Thierry Dargent, Richard Epenoy. Low-thrust Interplanetary Trajectories with Missed Thrust Events: a Numerical Approach. 2025. ⟨hal-05368349⟩

**HAL Id: hal-05368349**

**<https://hal.science/hal-05368349v1>**

Preprint submitted on 17 Nov 2025

**HAL** is a multi-disciplinary open access archive for the deposit and dissemination of scientific research documents, whether they are published or not. The documents may come from teaching and research institutions in France or abroad, or from public or private research centers.

L'archive ouverte pluridisciplinaire **HAL**, est destinée au dépôt et à la diffusion de documents scientifiques de niveau recherche, publiés ou non, émanant des établissements d'enseignement et de recherche français ou étrangers, des laboratoires publics ou privés.



HAL Authorization

# Low-thrust Interplanetary Trajectories with Missed Thrust Events: a Numerical Approach

Pierre Carpentier<sup>1</sup>, Jean-Philippe Chancelier<sup>2</sup>, Guy Cohen<sup>2</sup>, Thierry Dargent<sup>3</sup>, and  
Richard Epenoy<sup>4</sup>

<sup>1</sup>UMA, ENSTA Paris, IP Paris, France

<sup>2</sup>CERMICS, École nationale des ponts et chaussées, IP Paris, France

<sup>3</sup>Thales Alenia Space, France

<sup>4</sup>Centre National d'Études Spatiales, France

November 17, 2025

## Abstract

The problem under consideration is to drive a spatial vehicle to a target at a given final time while minimizing fuel consumption. This is a classical optimal control problem in a deterministic setting. However temporary stochastic failures of the engine may prevent reaching the target after the engine usage is recovered. Therefore, a stochastic optimal control problem is formulated under the constraint of ensuring a minimal probability of hitting the target. This problem is modeled, improved and finally solved by dualizing the probability constraint and using an Arrow-Hurwicz stochastic algorithm. Numerical results concerning an interplanetary mission are presented.

## 1 Introduction and motivation

The study described in this paper is the result of a scientific collaboration conducted between Cermics, UMA and both the French government agency CNES<sup>1</sup> and Thales Alenia Space<sup>2</sup>. The collaboration took place from December 2007 to December 2010.

### 1.1 Problem statement

The primary objective of this work is to address the planning of space rendez-vous missions, which can be formulated as optimal control problems with terminal equality constraints. The cost function typically reflects goals such as minimizing final time and/or fuel consumption. However, the optimal control solutions derived from such formulations are generally not “robust”. That is, if a temporary engine failure occurs — causing a deviation from the ideal trajectory — it may become very difficult or even impossible to satisfy the terminal constraints. To address this limitation, we propose an alternative approach in which the final equality constraints are replaced by a *constraint in probability*, based on a stochastic model of engine failure occurrence and duration. The objective is to compute a reference trajectory that ensures a successful rendez-vous with a specified probability, despite potential engine breakdowns. Naturally, this reference trajectory entails a certain loss of performance, as measured by the cost function, when compared to the ideal optimal solution. The aim is therefore to make the trade-off between performance and safety more explicit and quantifiable.

---

<sup>1</sup><https://cnes.fr>

<sup>2</sup><https://www.thalesalieniaspace.com>

In more detail, we consider an optimal control problem involving a spacecraft governed by differential equations. The control variable  $u$  represents the action of the propulsion system, and the objective is to minimize fuel consumption while reaching a target at a *given* final time  $t_f$ . This type of problem can be addressed using Pontryagin’s Minimum Principle, which yields an optimal control profile  $u(\cdot)$ . However, if a temporary engine failure occurs during the mission, the planned control is forced to zero for the duration of the failure. Once the engine recovers, the control must be recalculated based on the actual position at the time of recovery in an attempt to still reach the target despite the deviation. Yet, this may not always be feasible. More specifically, given a probabilistic model for the breakdown time  $\mathbf{T}_p$  and its duration  $\mathbf{T}_d$ , one can compute the probability of successfully reaching the target after the engine recovers. Unfortunately, this probability tends to be low if the spacecraft has strictly followed the nominal optimal (deterministic) trajectory up to the point of failure. As a result, to improve the chances of completing the rendez-vous successfully, the trajectory must be planned from the outset to account for the possibility of engine breakdowns.

## 1.2 Literature review

In the field of spacecraft trajectory optimization, the Conway’s reference book [8] presents a variety of both analytical and numerical approaches to trajectory optimization (see also the review papers [28] and [7] for more recent references). This book also contains some chapters devoted to low-thrust orbital transfer. On this last subject, the review article [18] focuses on available numerical approaches for solving low-thrust optimization problems, with a special emphasis of available tools to solve such problems.

Among the literature on low-thrust trajectory design, some papers address more specifically the issue of robustness. Indeed, guaranteeing performances such as safety and cost under random disturbances is a major concern in a space mission design. Such disturbances are either modeling errors (initial state, unmodeled disturbances) or unexpected events (engine failures) or thrust realization errors in magnitude and direction. Different methods have been proposed to deal with the difficulty induced by stochasticity. A framework for primer vector-based trajectory correction policy is proposed in [29]. The paper [31] investigates the use of Reinforcement Learning for low-thrust trajectories design in presence of noises and missed thrust events. In [19], the authors develop a stochastic sequential convex programming approach and apply it to an Earth-Mars transfer. In [14], the robust trajectory design problem is formulated in the stochastic optimal control framework, more precisely as a belief optimal control problem. The paper [27] deals with missed thrust events, that is, engine failures during a planned thrusting phase, that may render the mission unrecoverable. The authors develop a framework to assess the robustness of a given nominal low-thrust trajectory.

Finally, three papers specifically deal with the problem of engine failure of low-thrust propulsion spacecraft. In [30], the authors introduce a virtual swarm method whose idea is to simultaneously optimize the nominal trajectory together with recovery trajectories after simulated failure. Using the swarm, they control the longest amount of time a spacecraft may coast away from a nominal trajectory while still being able to reach a terminal target once engine operations are resumed (missed thrust recovery margin). The paper [24] investigates the use of expected thrust fraction to design space trajectories capable of resisting missed thrust events. The expected thrust fraction embeds the stochastic nature of missed thrust events into a deterministic optimal control problem, which allows for the use of computationally efficient optimal control solvers in the design of resilient trajectories. Finally, the title of the paper [20] “Designing robust low-thrust interplanetary trajectories subject to one temporary engine failure” clearly indicates the interest of the author for a problem very similar to the one we study here. We share the same preoccupation as [20]: similar modeling (stochastic optimization problem subject to probabilistic constraints), and similar ways to tackle the problem using stochastic approximation methods. However, we differ in the way we solve the problem: the control structure (number of thrust and coast arcs) is imposed in [20] and simplifying assumptions are made when solving the optimal control subproblems, whereas we solve the problem without simplification in this study. This said, [20] constitutes a significant contribution to directly accounting for engine failure in an interplanetary transfer.

### 1.3 Paper’s content

In Sect. 2 and Sect. 3, we present and improve the formulation of the problem of driving the satellite in an optimal way subject to meet the rendez-vous constraint with a given probability level. Starting from the “natural” optimization problem formulated using a probability constraint, we make use of several transformations in order to obtain a formulation adapted to numerical treatments. The deal is to finally obtain a stochastic optimization problem such that both the cost function and the final target constraint correspond to expectations.

In Sect. 4, we recall the stochastic gradient method and its application to an optimization problem subject to a constraint in expectation. We point out the main difficulties associated with the implementation of such an algorithm in the context of our rendez-vous problem. Indeed a stochastic estimate of the probability constraint gradient is not available here in a straightforward manner, and we have to use approximation techniques in order to obtain such an estimate. We detail the way convergence is affected by these approximations.

In Sect. 5, we use the previous approximation method to solve a real-life rendez-vous problem, and we present numerical results illustrating how the optimal deterministic control used before any failure is affected by the probability level associated with the target constraint. We also illustrate the trade-off safety (probability level) versus economic performance (fuel consumption).

Finally, we draw some conclusions in Sect. 6 and we point out some obstacles, both from the theoretical and the numerical point of view, we have to tackle for effectively solving such problems.

## 2 Problem formulation

In this section, we present the satellite model and the associated optimization problem, as well as the stochastic components that come into play in this problem.

### 2.1 Satellite model and deterministic problem

We consider a simplified dynamic model of a satellite, in which perturbation forces are neglected. The equations describing the satellite evolution are

$$\frac{dr}{dt} = v, \quad \frac{dv}{dt} = -\nu \frac{r}{\|r\|^3} + \frac{T}{m} \kappa, \quad \frac{dm}{dt} = -\frac{T}{g_0 I_{sp}} \delta. \quad (1)$$

The variables  $r \in \mathbb{R}^3$  and  $v \in \mathbb{R}^3$  are the inertial position and velocity of the satellite, and  $m \in \mathbb{R}$  is its mass. The variables which allow to control the satellite are  $\kappa \in \mathbb{R}^3$  (direction cosines of the thrust) and  $\delta \in \{0, 1\}$  (on-off switch of the engine). We suppose that the control  $\delta$  is relaxed in order to have a continuous control variable:  $\delta \in [0, 1]$ . These equations involve the constants  $\nu$  (gravitational constant),  $g_0$  (standard acceleration), as well as the specific impulse  $I_{sp}$  and the thrust<sup>3</sup>  $T$  of the engine.

The coordinates  $(r, v)$  have several drawbacks (delicate physical interpretation, impossible mathematical simplifications) so that it is preferable to use the so-called equinoctial coordinates to model the satellite dynamics. The coordinate change is described in Appendix A and leads to a satellite state variable  $x \in \mathbb{R}^7$  where  $(x_1, \dots, x_6) = (p, e_x, e_y, h_x, h_y, \ell)$  are the equinoctial coordinates of the satellite,  $x_7 = m$  being its mass. The satellite control variable  $u = (q, s, w) \in \mathbb{R}^3$  corresponds to the radial, tangential and normal components of the control.

The deterministic control problem we aim to solve is to drive the satellite from given initial conditions  $x_i \in \mathbb{R}^7$  at a given time  $t_i$  to a known final target, namely a position  $(x_{f,1}, \dots, x_{f,6})$ , at a given final time  $t_f$  while minimizing fuel consumption, that is  $m(t_i) - m(t_f) = (x(t_i) - x(t_f))_7$ . This optimal control problem is therefore stated with a predetermined final time. More precisely, the deterministic optimization problem is

---

<sup>3</sup>assumed constant rather than a function of the radius

formulated as

$$\min_u K(x(t_f)) , \quad (2a)$$

$$\text{s.t. } x(t_i) = x_i , \quad \frac{dx}{dt}(t) = f(x(t), u(t)) , \quad (2b)$$

$$\|u(t)\| \leq 1 \quad \forall t \in [t_i, t_f] , \quad (2c)$$

$$C(x(t_f)) = 0 , \quad (2d)$$

where mapping  $f$  is defined in Appendix A, the mapping  $K : x \in \mathbb{R}^7 \mapsto (x_i - x)_7$  is the final cost function giving the fuel consumption during the mission, and the mapping  $C : \mathbb{R}^7 \rightarrow \mathbb{R}^6$  describing the rendez-vous constraint is defined by

$$C : x \in \mathbb{R}^7 \mapsto (x_1 - x_{f,1}, \dots, x_6 - x_{f,6}) ,$$

where  $(x_{f,1}, \dots, x_{f,6})$  are the equinoctial coordinates corresponding to the final target  $(r_f, v_f)$ . Problem (2) is called a mission, and we say that the mission has failed if the target is not reached.

## 2.2 Satellite model with engine failure during a time interval

We want to take into account *engine failures* during the satellite mission. For that purpose we use a simplified failure model by assuming that there is *at most* one failure during a mission. Thus, a failure model consists in an oriented pair of two times  $(t_p, t_d)$ , where  $t_p$  is the time of the failure and  $t_d$  is the duration of the failure.

The dynamics of the satellite in the presence of failure is not different from that given by (2b), and is characterized by the fact that the control  $u$  is equal to 0 during the failure. To ease the description of the satellite dynamics, given two times  $s \leq s'$ , we introduce a flow map function  $\Phi_{s,s'}^u : \mathbb{R}^7 \rightarrow \mathbb{R}^7$  defined by

$$\begin{aligned} \Phi_{s,s'}^u : x \in \mathbb{R}^7 &\mapsto x^u(s') \\ \text{with } x^u(s) = x , \quad \frac{dx^u}{dt}(t) &= f(x^u(t), u(t)) , \quad \forall t \in [s, s'] . \end{aligned}$$

Now, assume that  $u$  is an admissible control for Problem 2. The satellite controlled dynamics under failure has now at most three different phases in the satellite dynamics.

1. During the time interval  $[t_i, t_p]$ , the nominal control  $u$ , which is defined over  $[t_i, t_f]$ , is used. It is an open-loop control, that is, a control that depends only on time  $t$ . The position of the satellite at the end of this first phase is

$$x_{t_p} = \Phi_{t_i, t_p}^u(x_i) .$$

2. During the time interval  $[t_p, t_p + t_d]$  the control is equal to 0 as the engine is not available. The position of the satellite at the end of the second phase is

$$x_{t_p + t_d} = \Phi_{t_p, t_p + t_d}^0(x_{t_p}) .$$

3. During the time interval  $[t_p + t_d, t_f]$ , we recover engine control and we can try to compute a recourse control  $v$  to achieve the mission of reaching the target. The position of the satellite at the end of the third phase is

$$x_{t_f} = \Phi_{t_p + t_d, t_f}^v(x_{t_p + t_d}) .$$

Now, gathering the three phases of the satellite dynamics the state of the satellite at final time  $t_f$  is given by

$$\Psi_{t_i, t_f}^{(u, v, t_p, t_d)}(x_i) = \begin{cases} \Phi_{t_i, t_f}^u(x_i) & \text{if } t_p \geq t_f , \\ \Phi_{t_p, t_f}^0(\Phi_{t_i, t_p}^u(x_i)) & \text{if } t_p < t_f \text{ and } t_p + t_d \geq t_f , \\ \Phi_{t_p + t_d, t_f}^v(\Phi_{t_p, t_p + t_d}^0(\Phi_{t_i, t_p}^u(x_i))) & \text{if } t_p < t_f \text{ and } t_p + t_d < t_f . \end{cases} \quad (3)$$

### 2.3 Engine failures and stochastic problem

As explained in §2.2, if an engine failure occurs, the satellite drifts away from the deterministic optimal trajectory. After the engine control is recovered, it is not always possible to drive the satellite to the final target. By anticipating such possible failures and by modifying the trajectory followed *before* any such failure occurs, one may increase the possibility of eventually reaching the target after a failure. But such a deviation from the deterministic optimal trajectory results in a decay of the economic performance.

We aim to formulate a new optimization problem where we need to balance the increased probability of achieving the mission (that is reaching the rendez-vous constraint) despite possible failures against the expected economic performance, that is, to quantify the price of safety one is ready to pay for.

There are different ways to accommodate these stochastic features in an optimization problem. The first possibility is to consider Robust Optimization (see [4] and the references therein for an overview of the subject). In this approach, the uncertainty model is not stochastic, but rather deterministic and set-based, in the sense that we seek for a solution that is feasible for any realization of the uncertainty in a given subset. Applied to our satellite problem, this approach aims to consider a failure subset  $\Xi_r$  (for example failures whose duration is less than or equal to a chosen value) and then at minimizing the cost associated with the “worst failure” while hitting the target for any failure in  $\Xi_r$ :

$$\begin{aligned} \min_u \min_v \quad & \left( \max_{(t_p, t_d) \in \Xi_r} K \left( \Psi_{t_i, t_f}^{(u, v, t_p, t_d)}(x_i) \right) \right), \\ \text{s.t.} \quad & C \left( \Psi_{t_i, t_f}^{(u, v, t_p, t_d)}(x_i) \right) = 0, \quad \forall (t_p, t_d) \in \Xi_r. \end{aligned}$$

We do not follow this direction and we rather appeal to Stochastic Optimization (see the reference books [25] and [26] for an overview). We consider a probability space  $(\Omega, \mathfrak{F}, \mathbb{P})$  and we assume given two random variables  $\mathbf{T}_p$  which is the time of the failure and  $\mathbf{T}_d$  which is the duration of the failure. It is assumed that  $\mathbf{T}_p$  and  $\mathbf{T}_d$  do not depend on the control  $u$ , which is possibly false in practice since engine failure may depend on how one drives the engine. Note that now, the recourse control  $v$  is a random variable as it is a recourse control which is computed knowing the two random variables  $\mathbf{T}_p$  and  $\mathbf{T}_d$ . As we adopt the convention to write random variables using capital bold letters, the recourse control  $v$  is renamed as  $\mathbf{V}$ . A natural criterion to be minimized in the stochastic formulation is the expectation of the final cost, so that the optimization problem sounds like:

$$\min_u \min_{\mathbf{V}} \mathbb{E} \left[ K \left( \Psi_{t_i, t_f}^{(u, \mathbf{V}, \mathbf{T}_p, \mathbf{T}_d)}(x_i) \right) \right].$$

It remains to define how to take the rendez-vous constraint into account.

- The first possibility is to formulate the constraint “almost surely”, which means that the target has to be reached for almost all failures according to the underlying probability law:

$$C \left( \Psi_{t_i, t_f}^{(u, \mathbf{V}, \mathbf{T}_p, \mathbf{T}_d)}(x_i) \right) = 0, \quad \mathbb{P}\text{-a.s.} \quad .$$

This formulation is however not relevant here because we know that there exist realizations of the failure such that the target cannot be reached whatever the deterministic control  $u$  used. The admissible set of the optimization problem is thus empty.

- The second possibility is to formulate the constraint in expectation:

$$\mathbb{E} \left[ C \left( \Psi_{t_i, t_f}^{(u, \mathbf{V}, \mathbf{T}_p, \mathbf{T}_d)}(x_i) \right) \right] = 0.$$

Such a formulation, although mathematically attractive, is not well-suited in this context because meeting the rendez-vous constraint in expectation still leaves the possibility that the target is not reached in (almost) any failure scenario, and, at the very least, this does not tell how many of those scenarios will hit the target. This leads us to the next formulation.

- The third possibility is to use a constraint in probability: in this setting, the target has not to be hit “almost always” as in the first possibility, but with a certain probability  $p$  whose value is given:

$$\mathbb{P}\left[C\left(\Psi_{t_i, t_f}^{(u, \mathbf{V}, \mathbf{T}_p, \mathbf{T}_d)}(x_i)\right) = 0\right] \geq p.$$

In the sequel, we concentrate on this last formulation in probability, which is particularly well suited for the optimization problem under consideration in this paper. As a matter of fact, we are here interested in a “death or life” process corresponding to the binary condition to reach the target or not,<sup>4</sup> and the probability constraint exactly does the work because it counts the scenarios in which the target is reached. Note that, while the robust approach focusses on the worst scenario in an a priori defined subset, this formulation amounts to considering the scenarios which are on the one hand feasible and on the other hand not too penalizing in terms of performance as measured by the cost function.

## 2.4 Initial stochastic formulation

To summarize what was said in §2.3, the first “natural” formulation of the optimal control problem under consideration consists in minimizing an expectation cost subject to a rendez-vous probability constraint:

$$\min_u \min_{\mathbf{V}} \mathbb{E}\left[K\left(\Psi_{t_i, t_f}^{(u, \mathbf{V}, \mathbf{T}_p, \mathbf{T}_d)}(x_i)\right)\right] \quad (4a)$$

$$\text{s.t. } \|u(t)\| \leq 1 \quad \forall t \in [t_i, t_f], \quad (4b)$$

$$\|\mathbf{V}(t)\| \leq 1 \quad \forall t \in [\mathbf{T}_p + \mathbf{T}_d, t_f], \quad (4c)$$

$$\mathbb{P}\left[C\left(\Psi_{t_i, t_f}^{(u, \mathbf{V}, \mathbf{T}_p, \mathbf{T}_d)}(x_i)\right) = 0\right] \geq p. \quad (4d)$$

Our main goal is to numerically solve this optimization problem. But Formulation (4) is not adapted to that purpose. First, the cost function takes all possible failures into account (by mean of the expectation operator), whereas we are in fact not interested in failures such that the satellite misses the target. Second, the probability constraint cannot be treated as is, and we need to find a more practical expression in order to numerically deal with it. Indeed, probability constraints raise important mathematical difficulties, such as the lack of convexity or connectedness of the feasible subset they induce. Those convexity or connectedness (or emptiness) properties depend of course on the properties of the function entering the constraint, but also on the probability distribution of the random variable and on the level  $p$  of probability required. One may refer to [21] and [22] for a general presentation of probability constraints, to [15] for connectedness properties, to [17] for convexity properties and to [16] for the question of stability (see also [26, Chap.4] for a review on optimization under probabilistic constraints). In this paper, we are mainly interested in the numerical difficulties arising when dealing with probability constraints. Thus we do not focus on theoretical questions and we assume that all the problems under consideration have the required properties when using numerical algorithms: connectedness and convexity of the admissible set, continuity and differentiability of the constraints and existence of saddle points for the Lagrangian associated to the problem.

In the next section, we modify and improve the formulation in order to obtain a numerically tractable optimization problem.

## 3 Formulation improvement

We now describe the improvements to be made to Problem (4) to obtain an operational formulation.

---

<sup>4</sup>Otherwise stated, the amount the target is missed does not matter if the target is not reached.

### 3.1 Expectation formulation

#### 3.1.1 Missing the target should not contribute to the cost function

When a failure occurs, it may be impossible for some cases to reach the target. For the other cases, depending on the required level  $p$  in the probability constraint (4d), one may decide not to reach the target even if possible. For all the failure scenarios such that the target is missed, the optimal control consists in not restarting the engine at the end of the failure because, as long as these scenarios contribute to the expected cost (4a), this is the way to reduce the fuel consumption. But we are in fact not interested in what happens whenever the mission fails, so that these scenarios yield an artificially good cost. Otherwise stated, a failure scenario, namely when the satellite misses the target and thus does not contribute to the probability constraint, should not be taken into account in the cost function. Thus we have to replace the original expected cost in (4a) by the expected cost *conditionally* to reaching the target, so that the problem becomes

$$\min_u \min_{\mathbf{V}} \mathbb{E} \left[ K \left( \Psi_{t_i, t_f}^{(u, \mathbf{V}, \mathbf{T}_p, \mathbf{T}_d)}(x_i) \right) \mid C \left( \Psi_{t_i, t_f}^{(u, \mathbf{V}, \mathbf{T}_p, \mathbf{T}_d)}(x_i) \right) = 0 \right] \quad (5a)$$

$$\text{s.t. (4b), (4c),} \quad (5b)$$

$$\mathbb{P} \left[ C \left( \Psi_{t_i, t_f}^{(u, \mathbf{V}, \mathbf{T}_p, \mathbf{T}_d)}(x_i) \right) = 0 \right] \geq p. \quad (5c)$$

#### 3.1.2 Probability as an expectation

Using standard properties of conditional expectation we rewrite Problem 5 as follows.

$$\min_u \min_{\mathbf{V}} \frac{\mathbb{E} \left[ K \left( \Psi_{t_i, t_f}^{(u, \mathbf{V}, \mathbf{T}_p, \mathbf{T}_d)}(x_i) \right) \times \mathbb{I}(\|C \left( \Psi_{t_i, t_f}^{(u, \mathbf{V}, \mathbf{T}_p, \mathbf{T}_d)}(x_i) \right)\|) \right]}{\mathbb{E} \left[ \mathbb{I}(\|C \left( \Psi_{t_i, t_f}^{(u, \mathbf{V}, \mathbf{T}_p, \mathbf{T}_d)}(x_i) \right)\|) \right]}, \quad (6a)$$

$$\text{s.t. (4b), (4c),} \quad (6b)$$

$$\mathbb{E} \left[ \mathbb{I}(\|C \left( \Psi_{t_i, t_f}^{(u, \mathbf{V}, \mathbf{T}_p, \mathbf{T}_d)}(x_i) \right)\|) \right] \geq p, \quad (6c)$$

where the real-valued indicator function  $\mathbb{I}$  is defined, for non negative values of  $y$ , by

$$\mathbb{I}(y) = \begin{cases} 1 & \text{if } y = 0, \\ 0 & \text{otherwise.} \end{cases} \quad (7)$$

**Remark 1** *The indicator function we introduced both in the cost function and in the probability constraint is highly discontinuous. Note however that the function  $\mathbb{I}$  is up to now inside an expectation so that we may recover smooth expressions once expectation is achieved.*

#### 3.1.3 Expectation based reformulation

In Problem (6), the denominator in the ratio defining the cost function is identical to the left-hand side of the constraint. This specificity allows us to use Lemma 5 in Appendix B, so that it is possible to replace the ratio defining the criterion (6a) by its numerator, provided that we a posteriori check a condition on the optimal multiplier associated with Constraint (6c). Instead of (6), we aim at solving the following problem for which both cost and constraint functions are expressed as expectations:

$$\min_u \min_{\mathbf{V}} \mathbb{E} \left[ K \left( \Psi_{t_i, t_f}^{(u, \mathbf{V}, \mathbf{T}_p, \mathbf{T}_d)}(x_i) \right) \times \mathbb{I}(\|C \left( \Psi_{t_i, t_f}^{(u, \mathbf{V}, \mathbf{T}_p, \mathbf{T}_d)}(x_i) \right)\|) \right] \quad (8a)$$

$$\text{s.t. (4b), (4c),} \quad (8b)$$

$$\mathbb{E} \left[ \mathbb{I}(\|C \left( \Psi_{t_i, t_f}^{(u, \mathbf{V}, \mathbf{T}_p, \mathbf{T}_d)}(x_i) \right)\|) \right] \geq p. \quad (8c)$$

With that reformulation, we have obtained a stochastic optimization problem formulation better suited to numerical resolution than the previous formulation (6), in the sense where both the criterion and the constraint correspond to expectations.

### 3.1.4 Introducing the no-failure scenario

The event  $\{\mathbf{T}_p \geq t_f\} \subset \Omega$  is called the “no-failure scenario”, because it corresponds to the set of failure scenarios that occur after the end of the mission. We denote by  $\pi_f$  the probability of that event, that is:

$$\pi_f = \mathbb{P}[\{\mathbf{T}_p \geq t_f\}] .$$

For every  $\omega \in \{\mathbf{T}_p \geq t_f\}$ , there is no need for a closed-loop control  $\mathbf{V}$ . Indeed, on the event  $\{\mathbf{T}_p \geq t_f\}$ , the state of the satellite at final time  $t_f$  only depends on the nominal control  $u$ .

For classical missions, we do hope that the probability  $\pi_f$  of the no-failure scenario is rather large (close to 1). Moreover, we expect the stochastic Problem (8) to have admissible solutions for some probability levels  $p$  higher than the probability  $\pi_f$  of the “no-failure scenario”. Therefore, we make the following assumption on  $p$  and  $\pi_f$ .

**Assumption 1** *The final time  $t_f$  and the probability level  $p$  of Problem (8) are such that*

$$p \geq \pi_f > \frac{1}{2} .$$

Under Assumption 1, we give in Lemma 2 an equivalent formulation of Problem (8). Moreover, one deduces from Lemma 2 that the optimal open-loop control used prior to any failure must be such that the associated state trajectory meets the rendez-vous constraint in the scenario without failure.

**Lemma 2** *Under Assumption 1, Problem (8) is equivalent to the following Problem (9)*

$$\min_u \min_{\mathbf{V}} \pi_f K(\Phi_{t_i, t_f}^u(x_i)) + (1 - \pi_f) \mathbb{E} \left[ K_I(\Psi_{t_i, t_f}^{(u, \mathbf{V}, \mathbf{T}_p, \mathbf{T}_d)}(x_i)) \mid \mathbf{T}_p < t_f \right] , \quad (9a)$$

$$s.t. \text{ (4b) , (4c) ,} \quad (9b)$$

$$\pi_f C(\Phi_{t_i, t_f}^u(x_i)) = 0 , \quad (9c)$$

$$(1 - \pi_f) \mathbb{E} \left[ I(\|C(\Psi_{t_i, t_f}^{(u, \mathbf{V}, \mathbf{T}_p, \mathbf{T}_d)}(x_i))\|) \mid \mathbf{T}_p < t_f \right] \geq p - \pi_f , \quad (9d)$$

where the function  $K_I$  is defined by  $K_I(\cdot) := K(\cdot) \times I(\|C(\cdot)\|)$ .

**Proof.** As a preliminary result, for any measurable mapping  $\varphi$ , we have that<sup>5</sup>

$$\begin{aligned} & \mathbb{E} \left[ \varphi \left( \Psi_{t_i, t_f}^{(u, \mathbf{V}, \mathbf{T}_p, \mathbf{T}_d)}(x_i) \right) \right] \\ &= \mathbb{E} \left[ \varphi \left( \Psi_{t_i, t_f}^{(u, \mathbf{V}, \mathbf{T}_p, \mathbf{T}_d)}(x_i) \right) \mathbf{1}_{\{\mathbf{T}_p \geq t_f\}} + \varphi \left( \Psi_{t_i, t_f}^{(u, \mathbf{V}, \mathbf{T}_p, \mathbf{T}_d)}(x_i) \right) \mathbf{1}_{\{\mathbf{T}_p < t_f\}} \right] \\ &= \mathbb{E} \left[ \varphi \left( \Phi_{t_i, t_f}^u(x_i) \right) \mathbf{1}_{\{\mathbf{T}_p \geq t_f\}} + \varphi \left( \Psi_{t_i, t_f}^{(u, \mathbf{V}, \mathbf{T}_p, \mathbf{T}_d)}(x_i) \right) \mathbf{1}_{\{\mathbf{T}_p < t_f\}} \right] \\ &= \pi_f \varphi \left( \Phi_{t_i, t_f}^u(x_i) \right) + (1 - \pi_f) \mathbb{E} \left[ \varphi \left( \Psi_{t_i, t_f}^{(u, \mathbf{V}, \mathbf{T}_p, \mathbf{T}_d)}(x_i) \right) \mid \{\mathbf{T}_p < t_f\} \right] . \end{aligned} \quad (10)$$

Now, applying Equality (10) with  $\varphi(\cdot) = I(\|C(\cdot)\|)$ , we obtain that Constraint (9c) can be equivalently rewritten as

$$\pi_f I(\|C(\Phi_{t_i, t_f}^u(x_i))\|) + (1 - \pi_f) \mathbb{E} \left[ I(\|C(\Psi_{t_i, t_f}^{(u, \mathbf{V}, \mathbf{T}_p, \mathbf{T}_d)}(x_i))\|) \mid \mathbf{T}_p < t_f \right] \geq p . \quad (11)$$

Then, we prove that (11) is equivalent to (9c) and (9d).

- First, it is immediate that the implication (9c)  $\wedge$  (9d)  $\implies$  (11) holds true. Indeed, assuming (9c), we have that  $I(\|C(\Phi_{t_i, t_f}^u(x_i))\|) = 1$  and then Inequality (9d) gives (11).

<sup>5</sup>with, for a set  $A$ , the notation  $\mathbf{1}_A(a) = 1$  if  $a \in A$  and  $\mathbf{1}_A(a) = 0$  otherwise

- Second, we prove the reverse implication (11)  $\implies$  (9c)  $\wedge$  (9d) by contradiction. Assume that (11) is satisfied and that  $C(\Phi_{t_i, t_f}^u(x_i)) \neq 0$ , that is,  $I(\|C(\Phi_{t_i, t_f}^u(x_i))\|) = 0$ . Then we obtain

$$(1 - \pi_f) \mathbb{E} \left[ I(\|\Psi_{t_i, t_f}^{(u, \mathbf{V}, \mathbf{T}_p, \mathbf{T}_d)}(x_i)\|) \mid \mathbf{T}_p < t_f \right] \geq p. \quad (12)$$

As the left-hand side of Equation (12) is smaller than  $1 - \pi_f$  and the right-hand side is greater than  $\pi_f$  using Assumption 1, we obtain that  $1 - \pi_f \geq \pi_f$  which contradicts Assumption 1. We have obtained that (11) implies (9c) and thus immediately (9d).

Finally, we consider the cost in (8a). Applying Equality (10) with  $\varphi = K_I$ , the cost function in (8a) can be rewritten as

$$\begin{aligned} & \mathbb{E} \left[ K(\Psi_{t_i, t_f}^{(u, \mathbf{V}, \mathbf{T}_p, \mathbf{T}_d)}(x_i)) \times I(\|\Psi_{t_i, t_f}^{(u, \mathbf{V}, \mathbf{T}_p, \mathbf{T}_d)}(x_i)\|) \right] \\ &= \pi_f K_I(\Phi_{t_i, t_f}^u(x_i)) + (1 - \pi_f) \mathbb{E} \left[ K_I(\Psi_{t_i, t_f}^{(u, \mathbf{V}, \mathbf{T}_p, \mathbf{T}_d)}(x_i)) \mid \mathbf{T}_p < t_f \right], \quad (\text{by (10)}) \\ &= \pi_f K(\Phi_{t_i, t_f}^u(x_i)) + (1 - \pi_f) \mathbb{E} \left[ K_I(\Psi_{t_i, t_f}^{(u, \mathbf{V}, \mathbf{T}_p, \mathbf{T}_d)}(x_i)) \mid \mathbf{T}_p < t_f \right], \quad (\text{using (9c)}) \end{aligned}$$

which gives (9a). The proof is complete.  $\square$

Introducing the no-failure scenario in the formulation of the stochastic optimization problem allows us to use the conditional probability law  $\mathbb{P}\{\cdot \mid \mathbf{T}_p < t_f\}$  instead of the initial probability law  $\mathbb{P}[\cdot]$ . As we aim at implementing a stochastic gradient algorithm for solving the problem (see forthcoming Sect. 4), it would not be wise to draw failure scenarios according to the initial law  $\mathbb{P}$ , since the single no-failure scenario alone carries a large probability mass  $\pi_f$ . By using the conditional law  $\mathbb{P}\{\cdot \mid \mathbf{T}_p < t_f\}$ , a failure occurring during the mission is drawn at each iteration of the stochastic gradient algorithm.

### 3.2 Final formulation obtained by smoothing indicator function I

A major challenge in the formulation (9) is how to deal with the indicator function I that isn't even continuous. Using the notion of mollifier introduced in [13], we replace in Problem (9) the function I by a smoother (in fact continuous) function  $I_r$  defined for non negative values of  $y$  and depending on a parameter  $r > 0$ , namely.

$$I_r(y) = \max \left\{ 0, 1 - \frac{y}{r} \right\}, \quad (14)$$

where the approximation  $I_r$  of I improves as  $r$  decreases. Finally, we consider the following smoothed Problem (15) derived from Problem (9):

$$\min_{u \in \mathcal{U}} \min_{\mathbf{V} \in \mathcal{V}} \pi_f K(\Phi_{t_i, t_f}^u(x_i)) + (1 - \pi_f) \mathbb{E} \left[ K_{I_r}(\Psi_{t_i, t_f}^{(u, \mathbf{V}, \mathbf{T}_p, \mathbf{T}_d)}(x_i)) \mid \mathbf{T}_p < t_f \right], \quad (15a)$$

$$\text{s.t. } \pi_f C(\Phi_{t_i, t_f}^u(x_i)) = 0, \quad (15b)$$

$$p - \pi_f - (1 - \pi_f) \mathbb{E} \left[ I_r(\|\Psi_{t_i, t_f}^{(u, \mathbf{V}, \mathbf{T}_p, \mathbf{T}_d)}(x_i)\|) \mid \mathbf{T}_p < t_f \right] \leq 0. \quad (15c)$$

$$\text{with } \mathcal{U} = \{u \mid \forall t \in [t_i, t_f], \|u(t)\| \leq 1\},$$

$$\mathcal{V} = \{\mathbf{V} \mid \forall t \in [\mathbf{T}_p + \mathbf{T}_d, t_f], \|\mathbf{V}(t)\| \leq 1\}.$$

## 4 Stochastic gradient algorithm

Formulation (15) consists in minimizing the expected cost (15a) subject to the constraint in expectation (15c). It is thus well suited for applying a stochastic gradient algorithm, namely the Arrow-Hurwicz algorithm, for finding a saddle point of the Lagrangian of Problem (15): see [9] for stochastic gradient methods with deterministic constraints, [11] and [10] when dealing with constraints in expectation in the sub-differentiable

case (see also [6, Chap 10] for a more recent reference, in French). In this section, we develop the practical implementation on the Arrow-Hurwicz algorithm. As already mentioned, we do not focus on theoretical questions and we assume that using such an algorithm can be justified in the present setting. The main assumption is in fact the existence of a saddle point for Problem (15), a difficult issue in the framework of probabilistic constraints.

## 4.1 Lagrangian formulation

Denoting by  $\mu \in \mathbb{R}^+$  the multiplier associated with Constraint (15c), the dual optimization problem we have to solve is

$$\max_{\mu \geq 0} \min_{u \in \mathcal{U}, \mathbf{V} \in \mathcal{V}} \pi_f K(\Phi_{t_i, t_f}^u(x_i)) + (1 - \pi_f) \mathbb{E} \left[ K_{I_r}^\mu(\Psi_{t_i, t_f}^{(u, \mathbf{V}, \mathbf{T}_p, \mathbf{T}_d)}(x_i)) \mid \mathbf{T}_p < t_f \right], \quad (16a)$$

$$\text{s.t. } \pi_f C(\Phi_{t_i, t_f}^u(x_i)) = 0, \quad (16b)$$

with the notation  $K_{I_r}^\mu(\cdot) = (K(\cdot) - \mu) \times I_r(\cdot)$ . The minimization with respect to the closed-loop strategy  $\mathbf{V}$  and the conditional expectation can be interchanged (see [23, Theorem 14.60] for mathematical details): loosely speaking, there are as many closed-loop controls as scenarios, so that the minimization with respect to the closed-loop strategy is in fact achieved scenario by scenario. Therefore Problem (16) is equivalent to the following dual problem:

$$\max_{\mu \geq 0} \min_{u \in \mathcal{U}} \pi_f K(\Phi_{t_i, t_f}^u(x_i)) + (1 - \pi_f) \mathbb{E} \left[ \min_{\mathbf{V} \in \mathcal{V}} K_{I_r}^\mu(\Psi_{t_i, t_f}^{(u, \mathbf{V}, \mathbf{T}_p, \mathbf{T}_d)}(x_i)) \mid \mathbf{T}_p < t_f \right], \quad (17a)$$

$$\text{s.t. } \pi_f C(\Phi_{t_i, t_f}^u(x_i)) = 0. \quad (17b)$$

This dual problem incorporates an optimization problem in  $\mathbf{V}$ , whose optimal value depends on the no-failure scenario only by means of the state value  $x_{\mathbf{T}_p}^u = \Phi_{t_i, \mathbf{T}_p}^u(x_i)$ . Indeed, using the fact that we only consider events in  $\{\mathbf{T}_p < t_f\}$ , the value of function  $\Psi$  in Equation (3) is rewritten as

$$\Psi_{t_i, t_f}^{(u, \mathbf{V}, \mathbf{T}_p, \mathbf{T}_d)}(x_i) = \Gamma_{\mathbf{T}_p, t_f}^{\mathbf{V}, \mathbf{T}_d}(\Phi_{t_i, \mathbf{T}_p}^u(x_i)) \quad (18a)$$

$$\text{with } \Gamma_{\mathbf{T}_p, t_f}^{\mathbf{V}, \mathbf{T}_d} : x \mapsto \begin{cases} \Phi_{\mathbf{T}_p, t_f}^0(x) & \text{if } \mathbf{T}_p + \mathbf{T}_d \geq t_f, \\ \Phi_{\mathbf{T}_p + \mathbf{T}_d, t_f}^{\mathbf{V}}(\Phi_{\mathbf{T}_p, \mathbf{T}_p + \mathbf{T}_d}^0(x)) & \text{if } \mathbf{T}_p + \mathbf{T}_d < t_f, \end{cases} \quad (18b)$$

and we rewrite Problem (17) as

$$\max_{\mu \geq 0} \min_{u \in \mathcal{U}} \pi_f K(\Phi_{t_i, t_f}^u(x_i)) + (1 - \pi_f) \mathbb{E} \left[ W_r(\Phi_{t_i, \mathbf{T}_p}^u(x_i), \mathbf{T}_p, \mathbf{T}_d, \mu) \mid \mathbf{T}_p < t_f \right], \quad (19a)$$

$$\text{s.t. } \pi_f C(\Phi_{t_i, t_f}^u(x_i)) = 0, \quad (19b)$$

where the mapping  $W_r(x, t_p, t_d, \mu)$  is defined by

$$W_r(x, t_p, t_d, \mu) = \min_v (K(\Gamma_{t_p, t_f}^{v, t_d}(x)) - \mu) I_r(\|C(\Gamma_{t_p, t_f}^{v, t_d}(x))\|). \quad (20)$$

Problem (20) is hereafter called the *internal problem*. Assuming that the function  $W_r$  can be computed for any given sample of the random variables  $\mathbf{T}_p$  and  $\mathbf{T}_d$ , we observe that the *external* max-min problem (19) now involves only deterministic variables  $\mu$  and  $u$ .

## 4.2 Stochastic Arrow-Hurwicz algorithm

The Arrow-Hurwicz algorithm consists in alternating gradient steps performed on the primal decision variable and on the dual variable associated with a dualized constraint. The algorithm, first introduced in [3] in the

deterministic framework, has been extended to the stochastic case with deterministic constraint (see [9]) and with constraint in expectation (see [11], proofs in [10]). In the latter case, one considers the problem

$$\min_{u \in U^{\text{ad}}} \mathbb{E} [j(u, \boldsymbol{\xi})] \quad \text{s.t.} \quad \mathbb{E} [\theta(u, \boldsymbol{\xi})] \leq 0 ,$$

where  $u$  is a deterministic control (open-loop) and  $\boldsymbol{\xi}$  is a random variable with given probability law. Then the  $k$ -th iteration of the stochastic Arrow-Hurwicz algorithm consists in drawing a sample  $\xi^k$  of  $\boldsymbol{\xi}$  and updating the primal variable  $u$  and the dual variable  $\mu$  by (sub-)gradients steps, namely,

$$\begin{aligned} u^{k+1} &= \text{proj}_{U^{\text{ad}}} \left( u^k - \epsilon_u^k \nabla_u (j(u^k, \xi^k) + \mu^k \theta(u^k, \xi^k)) \right) , \\ \mu^{k+1} &= \max \{ 0, \mu^k + \epsilon_\mu^k \theta(u^k, \xi^k) \} , \end{aligned}$$

where  $\epsilon_u^k$  and  $\epsilon_\mu^k$  are infinite sequences of numbers such that

$$\epsilon^k > 0 , \quad \sum_{k=0}^{+\infty} \epsilon^k = +\infty , \quad \sum_{k=0}^{+\infty} (\epsilon^k)^2 < +\infty .$$

Here we consider Problem (15) and its dual reformulation (19). At iteration  $k$  of the stochastic Arrow-Hurwicz algorithm, we have at our disposal current values  $u^k$  for the control,  $x^k$  for the state of the no-failure scenario,  $\mu^k$  for the multiplier,  $r^k$  for the smoothing coefficient,  $\epsilon_u^k$  and  $\epsilon_\mu^k$  for the gradient step lengths. The iteration consists of the following steps.

- (1) Draw a failure scenario  $\xi^k = (t_p^{\xi^k}, t_d^{\xi^k})$  according to the conditional probability law  $\mathbb{P}\{\cdot | t_p^{\xi^k} \leq t_f\}$ .
- (2) Compute the partial (sub-)gradient  $\nabla_x W_{r,k}(x^k(t_p^{\xi^k}), t_p^{\xi^k}, t_d^{\xi^k}, \mu^k)$  with respect to  $x$  and the partial (sub-)gradient  $\nabla_\mu W_{r,k}(x^k(t_p^{\xi^k}), t_p^{\xi^k}, t_d^{\xi^k}, \mu^k)$  with respect to  $\mu$  of the function  $W_{r,k}$  (defined in Equation (20)), optimal cost of the inner optimization problem.
- (3) In backward time, compute the adjoint state  $\lambda^k(\cdot)$  on  $[t_p^{\xi^k}, t_f]$ :

$$\lambda^k(t_f) = \pi_f \nabla K(x^k(t_f)) , \quad \frac{d\lambda^k}{dt}(t) = \nabla_x f(x^k(t), u^k(t))^\top \lambda^k(t) .$$

- (4) At time  $t_p^{\xi^k}$ , incorporate the jump induced by the cost term  $(1 - \pi_f)W_{r,k}$ :

$$\lambda_-^k(t_p^{\xi^k}) = \lambda^k(t_p^{\xi^k}) + (1 - \pi_f) \nabla_x W_{r,k}(x^k(t_p^{\xi^k}), t_p^{\xi^k}, t_d^{\xi^k}, \mu^k) .$$

- (5) In backward time, compute the adjoint state  $\lambda^k(\cdot)$  on  $[t_i, t_p^{\xi^k}]$  starting from the initial value  $\lambda_-^k(t_p^{\xi^k})$ .
- (6) Compute the partial (sub-)gradient  $\nabla_u H(x^k(\cdot), u^k(\cdot), \lambda^k(\cdot))$  with respect to  $u$  of the Hamiltonian  $H(x, u, \lambda) = \lambda^\top f(x, u)$ , and update the control  $u$  by performing a descent gradient step projected on the intersection of the unit ball  $S_1 = \{u | \|u(t)\| \leq 1, \forall t\}$  and the subset  $C_{\text{ad}} = \{u | C(x(t_f)) = 0\}$  of controls to reach the final target:

$$u^{k+1}(\cdot) = \text{proj}_{S_1 \cap C_{\text{ad}}} \left( u^k(\cdot) - \epsilon_u^k \nabla_u H(x^k(\cdot), u^k(\cdot), \lambda^k(\cdot)) \right) .$$

- (7) Update the dual variable  $\mu$  by performing a gradient ascent step:

$$\mu^{k+1} = \text{proj}_{\mathbb{R}^+} \left( \mu^{(k)} + \epsilon_\mu^k (p - \pi_f + (1 - \pi_f) \nabla_\mu W_{r,k}(x^k(t_p^{\xi^k}), t_p^{\xi^k}, t_d^{\xi^k}, \mu^k)) \right) .$$

- (8) Compute in forward time the state  $x^{k+1}(\cdot)$  on  $[t_i, t_f]$ :

$$x^{k+1}(t_i) = x_i , \quad \frac{dx^{k+1}}{dt}(t) = f(x^{k+1}(t), u^{k+1}(t)) .$$

The main outputs of the algorithm are the optimal state trajectory  $x^*$  and control trajectory  $u^*$  for the no-failure scenario.

**Remark 3** *As will be explained in §4.3, the target constraint  $C(x(t_f)) = 0$  is treated by duality when solving the inner problem in order to compute  $W_{r,k}(x^k(t_p^{\xi^k}), t_p^{\xi^k}, t_d^{\xi^k}, \mu^k)$  and its partial (sub-)gradients. By contrast, in the stochastic Arrow-Hurwicz algorithm described above, the target constraint  $C(x(t_f)) = 0$  associated with the no-failure scenario is treated by projection. The reason for that is that dualizing this last target constraint has led in our numerical experiments to an instable behavior of the stochastic Arrow-Hurwicz algorithm for high probability level  $p$ . Note that the projection on the intersection  $S_1 \cap C_{\text{ad}}$  involves the resolution of an optimal control problem. Indeed, using the notation  $u^{k+\frac{1}{2}}(\cdot) = u^k(\cdot) - \epsilon_u^k \nabla_u H(x^k(\cdot), u^k(\cdot), \lambda^k(\cdot))$ , this projection amounts to solving:*

$$\min_u \frac{1}{2} \int_{t_i}^{t_f} \|u(t) - u^{k+\frac{1}{2}}(t)\|^2 dt \quad (21a)$$

$$\text{s.t. } x(t_i) = x_i, \quad \frac{dx}{dt}(t) = f(x(t), u(t)), \quad (21b)$$

$$\|u(t)\| \leq 1 \quad \forall t \in [t_i, t_f], \quad (21c)$$

$$C(x(t_f)) = 0. \quad (21d)$$

*This problem is well conditioned and can be easily solved using an adapted optimal control algorithm such as the one used to solve the inner problem (see §4.3).*

In summary, one iteration of the stochastic Arrow-Hurwicz algorithm aims at solving two deterministic optimal control problems:

- Problem (20) for computing the optimal value  $W_{r,k}(x^k(t_p^{\xi^k}), t_p^{\xi^k}, t_d^{\xi^k}, \mu^k)$  and the associated derivatives,
- Problem (21) for computing the projection on  $S_1 \cap C_{\text{ad}}$ .

In the next section, we detail the way Problem (20) is treated.

### 4.3 A heuristic for solving the inner Problem (20)

As just explained in §4.2, at each iteration of the stochastic Arrow-Hurwicz algorithm, we have to compute  $W_{r,k}(x^k(t_p^{\xi^k}), t_p^{\xi^k}, t_d^{\xi^k}, \mu^k)$  which is the optimal value of the deterministic inner optimal control problem (20), as well as its partial (sub-)gradient. To perform that task, given  $(x, t_p, t_d, \mu) = (x^k(t_p^{\xi^k}), t_p^{\xi^k}, t_d^{\xi^k}, \mu^k)$ , we have to solve the optimal control problem:

$$\min_v (K(x(t_f)) - \mu) I_r(\|C(x(t_f))\|), \quad (22a)$$

$$\text{s.t. } x(t_p) = x, \quad \frac{dx}{dt}(t) = f(x(t), v(t)), \quad (22b)$$

$$\begin{aligned} v(t) &= 0 \quad \forall t \in [t_p, t_p + t_d], \\ \|v(t)\| &\leq 1 \quad \forall t \in [t_p + t_d, t_f]. \end{aligned} \quad (22c)$$

Problem (22) is difficult to tackle numerically because, for a control  $v$  that does not bring the final state constraint into a ball of radius  $r$  (assumed to be or to become small), the associated cost is zero, as is its sensitivity to the control. For that reason, in order to obtain a numerical solution of Problem (22), we solve the optimal control problem of minimizing the final cost under the constraint of hitting the target exactly, that is,

$$\min_v K(x(t_f)) - \mu, \quad (23a)$$

$$\text{s.t. } (22b), (22c), \text{ and} \quad (23b)$$

$$C(x(t_f)) = 0, \quad (23c)$$

using the deterministic Arrow-Hurwicz algorithm [3], where the final constraint (23c) is dualized using an *augmented Lagrangian*<sup>6</sup> in the algorithm. The deterministic Arrow-Hurwicz algorithm produces a sequence  $\{\delta^\kappa\}_{\kappa \in \mathbb{N}}$  where  $\delta^\kappa$  is the deviation  $C(x(t_f))$  from target at iteration  $\kappa$ , and a sequence  $\{v^\kappa\}_{\kappa \in \mathbb{N}}$  where  $v^\kappa$  is the multiplier associated with the final constraint (23c) at iteration  $\kappa$ . Several cases have to be considered when solving Problem (23).

1. The sequence  $\{\delta^\kappa\}_{\kappa \in \mathbb{N}}$  does not stabilize: we consider that the algorithm diverges.
2. The sequence  $\{\delta^\kappa\}_{\kappa \in \mathbb{N}}$  converges to  $\delta^*$ :
  - (a) if  $\|\delta^*\| = 0$ , the final target constraint is satisfied, the algorithm converges to a solution with a final state  $x^*(t_f)$ :
    - if  $K(x^*(t_f)) - \mu \geq 0$ , the solution of Problem (22) is to do nothing (see postponed Lemma 4),
    - otherwise, the solution of Problem (22) is very similar to the solution of Problem (23) since we are as close as possible to the target (see Appendix D), and the optimal value  $v^*$  of the multiplier allows to compute the derivatives of  $W_r$  used in the stochastic Arrow-Hurwicz algorithm,
  - (b) otherwise, the target cannot be reached and  $\|\delta^*\|$  is the distance by which the target is missed: the sequence of multipliers  $\{v^\kappa\}_{\kappa \in \mathbb{N}}$  goes to infinity and the deterministic Arrow-Hurwicz algorithm aims to get as close as possible to the final target, with a final state  $x^*(t_f)$ :
    - if  $K(x^*(t_f)) - \mu \geq 0$ , the solution of Problem (22) is to do nothing,
    - if  $\|\delta^*\| > r$ , the solution of Problem (22) is to do nothing,
    - otherwise, the solution of Problem (23) is the solution of Problem (22).

Note that the deterministic Arrow-Hurwicz algorithm used to solve Problem (23) takes the distinctions made in Appendix D concerning the study of Problem (22) into account, that is, the case where the target is exactly reached has to be treated separately of the case where the target is reached up to  $r$ . So far, we do not have formal proof of the equivalence suggested above between Problems (22) and (23). This is an area where progress should be made.

From the expression of the criterion (22a) and the shape of  $I_r$  given by (14), we deduce Lemma 4 used in the heuristic description.

**Lemma 4** *Let  $(x^*, v^*)$  be an optimal solution of the inner problem (22) and assume that the optimal solution is such that  $\|C(x^*(t_f))\| < r$  so that  $I_r$  is non zero. Then, we have that*

$$K(x^*(t_f)) - \mu \leq 0. \quad (24)$$

**Proof.** Indeed, ▶ en fait c'est une hypothèse raisonnable mais pas impliqué ◀ it is always possible to miss the target and thus to obtain a cost equal to 0 thanks to the indicator function, so that  $K(x^*(t_f)) - \mu > 0$  cannot induce an optimal cost in (22). □

#### 4.4 Parameters of the stochastic Arrow-Hurwicz algorithm

As indicated in §4.2, some parameters have to be chosen when implementing the stochastic Arrow-Hurwicz algorithm. As with any standard stochastic gradient algorithm, the step lengths  $\epsilon_u^k$  and  $\epsilon_\mu^k$  must be properly set. According to the theory (see [11]), these parameters should vary in  $1/k$  and therefore be of the general form:

$$\frac{\alpha}{\beta + k}. \quad (25)$$

---

<sup>6</sup>that is, additional duality terms  $\nu^\top C(x(t_f)) + \frac{\epsilon}{2} \|C(x(t_f))\|^2$

In order to properly set the smoothing coefficient  $r^k$ , we get inspiration from [2] (with proofs in the companion paper [1]), where a general problem of minimizing a criterion in expectation under a probability constraint is studied. As a result, the smoothing coefficient at iteration  $k$  of the stochastic Arrow-Hurwicz algorithm is chosen as (see details in Appendix C)

$$r^k = \frac{a}{b + k^{1/3}} . \quad (26)$$

Note that such a smoothing coefficient (in  $k^{-1/3}$ ) is divided by 10 after 1000 iterations, and by 100 after  $10^6$  iterations.

## 5 Real-life application

In this section, we describe the specific problem we addressed in this study and give numerical results for different probability levels required for hitting the target.

### 5.1 Problem data

The numerical data (see §2.1) corresponding to the spatial mission that we study in this paper can be found in [12]. They involve a rescaling for proper numerical treatment and are as follows.

- Parameter:<sup>7</sup>

$$T = 0.0336750 , \quad g_0 I_{\text{sp}} = 0.4936891 , \quad \nu = 1 .$$

- Initial and final times:<sup>8</sup>

$$t_i = 0.6888699 , \quad t_f = 8.7830909 .$$

- Satellite initial state:<sup>9</sup>

$$x_i = (0.999702 \quad -0.003359 \quad 0.016942 \quad -0.000011 \quad 0.000007 \quad 36.52939 \quad 1)^T .$$

- Rendez-vous target coordinates:

$$(x_{f,1} \quad x_{f,2} \quad x_{f,3} \quad x_{f,4} \quad x_{f,5} \quad x_{f,6}) = (1.511514 \quad 0.085367 \quad -0.037923 \quad 0.010474 \quad 0.012275 \quad 42.17610) .$$

- Failure probability laws

The instant at which the failure occurs and the failure duration follow exponential probability laws, whose parameters are

- failure start time:  $t_p = 0.68887$  and  $\lambda_p = 15.1711$ ,
- failure duration:  $t_d = 0.03444$  and  $\lambda_d = 0.05350$ .

Then, the probability weight  $\pi_f$  of the no-failure scenario is:

$$\pi_f = 0.58653 . \quad (27)$$

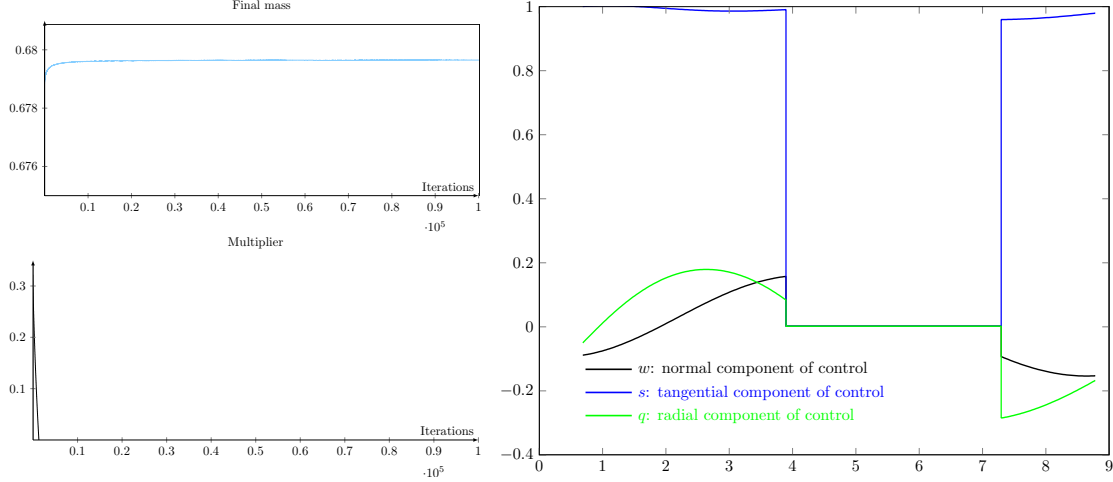


Figure 1: Convergence and solution of the deterministic problem

## 5.2 Deterministic problem solution

The convergence of the deterministic Arrow-Hurwicz algorithm as well as the optimal control obtained are depicted Figure 1.

In the deterministic solution, we distinguish three periods in the mission duration:

- period (a): engine at maximum thrust (between days 40 and 226.3),
- period (b): engine stopped (between days 226.3 and 423.8),
- period (c) : engine at maximum thrust (between days 423.8 and 510).

After scaling, the values of the instants delimiting these three periods are:

$$t_i = 0.68887 \text{ (initial time),}$$

$$t_a \approx 3.8983 \text{ (end of period (a)),}$$

$$t_b \approx 7.2980 \text{ (end of period (b)),}$$

$$t_f = 8.78309 \text{ (final time).}$$

These notations will be used when analyzing the results of the stochastic Arrow-Hurwicz algorithm.

It is easy to prove that a failure occurring before the end of period (a) does not prevent from reaching the target. Furthermore, a failure occurring during period (b) has no effect since the engine is stopped. The probability weight  $\pi_r$  that a failure occurs before the end of period (b) is:

$$\pi_r \approx 0.35020 .$$

Finally, the probability weight  $p^{\text{det}}$  of reaching the target when applying the deterministic optimal control is

$$p^{\text{det}} = \pi_f + \pi_r \approx 0.93673 . \quad (28)$$

<sup>7</sup>Before scaling, the parameters  $T$ ,  $g_0$  and  $I_{sp}$  are 0.2, 9.80665 and 1500 respectively.

<sup>8</sup>Before scaling, the initial and final times are 40 and 510 days respectively.

<sup>9</sup>Before scaling, the initial mass  $x_{i,7}$  of the satellite is 1000 kilograms.

### 5.3 Stochastic problem solutions for various probability values

We recall that each iteration of the stochastic Arrow-Hurwicz algorithm mainly consists in solving

- the deterministic optimal control problem associated with the inner problem,
- the deterministic optimal control problem associated with the projection.

On an Intel Core2 Quad CPU 2.83 Ghz computer running Linux, the CPU time associated with the resolution of these two problems is around 2.2 seconds. In all the numerical tests carried out in this study, the stochastic Arrow-Hurwicz algorithm is initialized with the deterministic optimal control trajectory, and an initial value of the multiplier  $\mu$  equal to 0.325. The stochastic Arrow-Hurwicz algorithm is stopped after 100,000 iterations.

#### 5.3.1 Numerical tests with a low probability level $p$

To begin with, we are interested in probability levels  $p$  that are strictly lower than the probability  $p^{\text{det}}$  to reach the target when using the deterministic solution. We observe (see Figure 2) that the algorithm converges very satisfactorily.

- For the probability level  $p = 0.550$ , that is, less than the probability of the no-failure scenario  $\pi_f$  (see (27)), the control trajectories of the no-failure scenario are identical to those of the deterministic optimal solution; the probability constraint is not active (multiplier equal to 0 since  $\pi_f > 0.550$ ) and the optimal fuel consumption is 0.32024.
- For the probability level  $p = 0.750$ , the convergence is more turbulent than in the previous case; the optimal fuel consumption of the no-failure scenario is slightly higher than in the previous case (0.32045), whereas the multiplier stabilizes around the value 0.3208. However the control trajectories obtained in this case are rather different from those associated with the no-failure problem, the main difference being located after instant  $t_b$  when a reduction of the engine speed appears.
- For the probability level  $p = 0.925$ , the optimal fuel consumption of the no-failure scenario is 0.32054, whereas the multiplier stabilizes around the value 0.3233, that is, a small difference with respect to the previous two cases. The control distortion after instant  $t_b$  is more pronounced than in the previous case, with very little impact on the optimal consumption.

One might think that the optimal control for the problem under probability constraint is identical to the optimal control in the deterministic case as soon as the probability level  $p$  is less than  $p^{\text{det}}$  in (28). In fact, this is not the case: the optimal control of the deterministic problem is just *admissible* for the stochastic optimization problem, because the two problems have different cost functions.

#### 5.3.2 Numerical tests with a medium probability level $p$

We are then interested in probability levels  $p$  that are slightly higher than the probability  $p^{\text{det}}$  to reach the target when using the deterministic solution. We observe (see Figure 3) that the algorithm still converges very satisfactorily.

- For the probability level  $p = 0.950$ , the solution behavior is very close to that observed in §5.3.1 for the probability level  $p = 0.925$  : the optimal fuel consumption is 0.3206 and the multiplier stabilizes around the value 0.3254.
- For a probability level  $p = 0.960$ , the optimal control of the no-failure scenario and the associated fuel consumption do not differ from those obtained for  $p = 0.960$ . But the optimal multiplier increases significantly, and its evolution during the algorithm is particularly slow during the first 40,000 iterations.

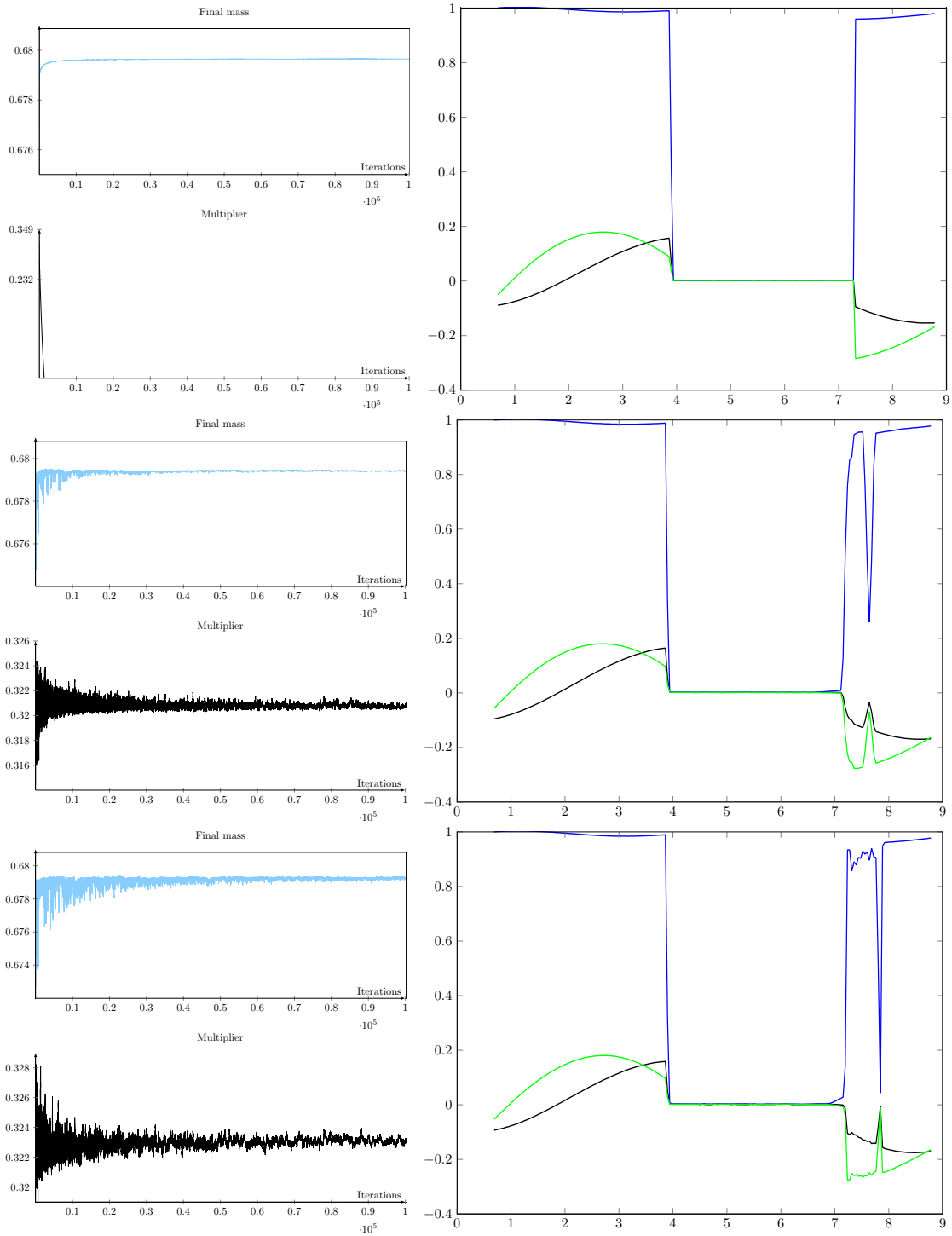


Figure 2: Results for  $p = 0.550$  (top),  $p = 0.750$  (middle) and  $p = 0.925$  (bottom)

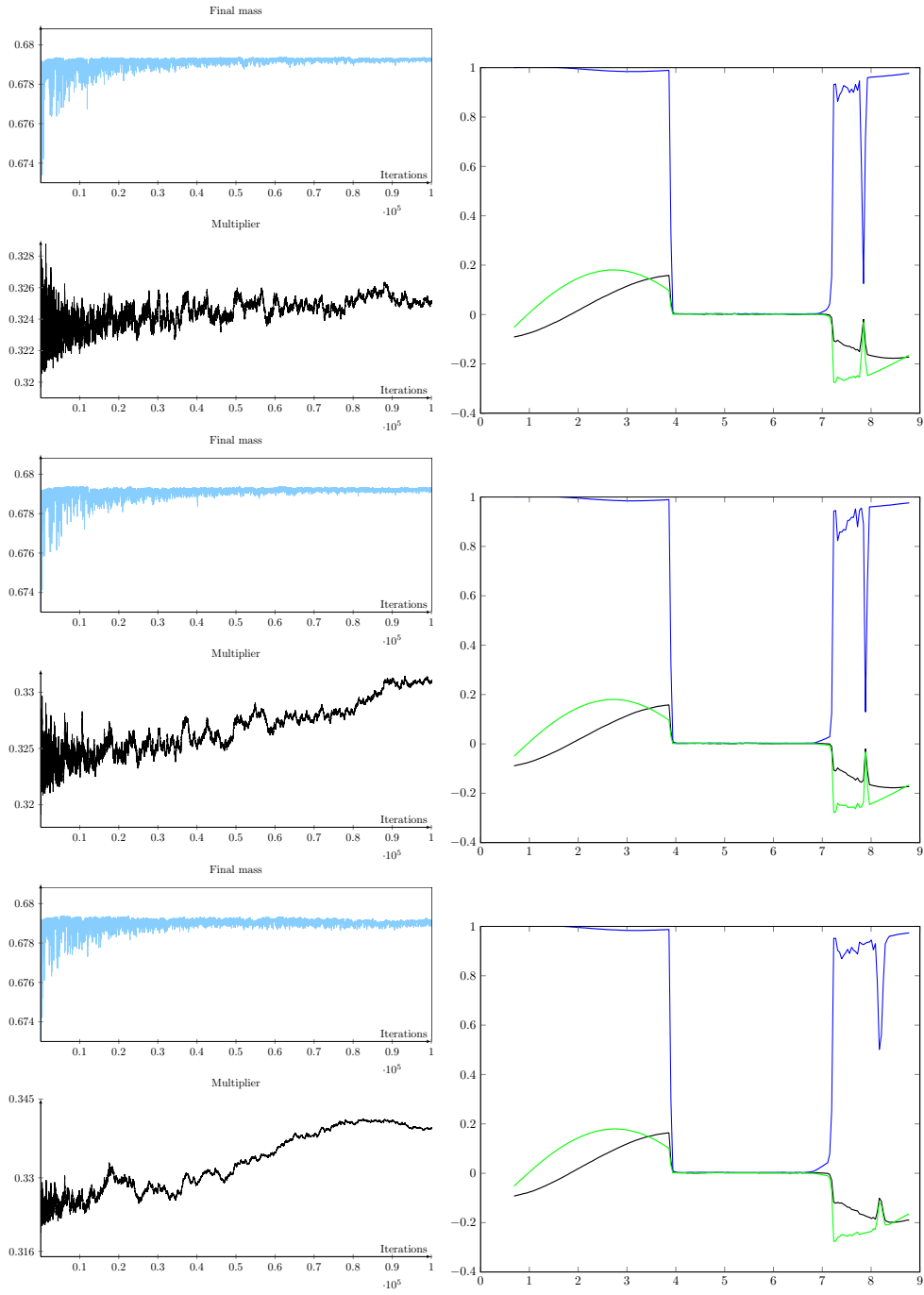


Figure 3: Results for  $p = 0.950$  (top),  $p = 0.960$  (middle) and  $p = 0.970$  (bottom)

- Finally, for the probability level  $p = 0.970$ , the multiplier increase over the iterations is even more impressive. The optimal control of the no-failure scenario also changes, the reduction of the engine speed after time  $t_b$  occurring later than in previous cases.

For those medium values of the probability level, we can see that satisfying the probability constraint is made possible by two actions involved simultaneously.

1. On the one hand, the increase in the multiplier means that fewer and fewer failures are being rejected for consumption reasons (remember that the term  $K(x^\xi(t_f)) - \mu$  must remain negative for a failure to be recovered): during the last 10,000 iterations of the stochastic Arrow-Hurwicz algorithm, that is, when the algorithm is almost stabilized, the number of failures eliminated for this reason drops from 250 for  $p = 0.950$  to 6 for  $p = 0.970$ .
2. On the other hand, the later the engine speed is reduced during the last period (c) of the mission, the more failures can be recovered, since any failure occurring between time  $t_b$  and the time corresponding to this speed reduction time can be recovered.

### 5.3.3 Numerical tests with a high probability level $p$

We are now interested in probability levels  $p$  that are significantly higher than the probability  $p^{\text{det}}$  to reach the target when using the deterministic solution, namely,  $p = 0.980$ ,  $p = 0.985$  and  $p = 0.990$ . The results are presented at Figure 4.

The results obtained for the medium probability levels are confirmed by these new numerical experiments. Surprisingly, the convergence of the multiplier  $\mu$  associated with the probability constraint seems easier to achieve than in the case of medium probability levels. As far as optimal control for the no-failure scenario is concerned, delaying the decrease in engine speed more and more as  $p$  increases (until the final instant  $t_f$  is reached) is clearly highlighted.

So it seems that the overall algorithm works reasonably well, but several improvements would still be desirable. These include the fact that a few tens of thousands of iterations at the start of the algorithm do not seem to provide much improvement, and it would be worth digging a little deeper to see if they could be dispensed with. If we add to this the fact that the computation time of an iteration is a little over 2 seconds for solving both the inner problem and the projection problem, and therefore that an execution of the algorithm requires a CPU time of the order of two and a half days, we understand that there is also a stake in finding a more efficient method of solving, for example shooting methods [5].

### 5.3.4 Numerical tests with an extreme probability level $p$

Finally, we are interested in “extreme” probability levels  $p$ , that is, allowing to reach the target for 99.5% and 99.9% of failures. The results are presented at Figure 5.

The results show that the dual variable  $\mu$  has not converged and continues to grow after 100,000 iterations. This is confirmed by the fact that the real probability of recovering a failure at the end of each run of the algorithm (respectively 99.3% and 99.6%) are a little lower than the probability levels requested. In the case of  $p = 0.999$ , we might even ask whether such a probability is feasible. In fact, it is not yet possible to determine the probability level above which the problem can no longer be solved. If we look at the shape of the optimal control along the no-failure scenario, we see the following new phenomenon: the restart of the engine after period (b) occurs earlier than in the case of high probability level in §5.3.3, this renewed activity before  $t_b$  being compensated by a reduction of the engine speed a little after  $t_b$  (as before, there is a sharp speed reduction just before the final instant  $t_f$ ). This is most probably how the algorithm tries to achieve the required probability level, but this is still to be confirmed.

## 5.4 Result summary

To conclude, as a function of the requested level of probability  $p$ , we present two graphics showing the variation of the optimal multiplier associated with the constraint on the one hand, and the variation of the

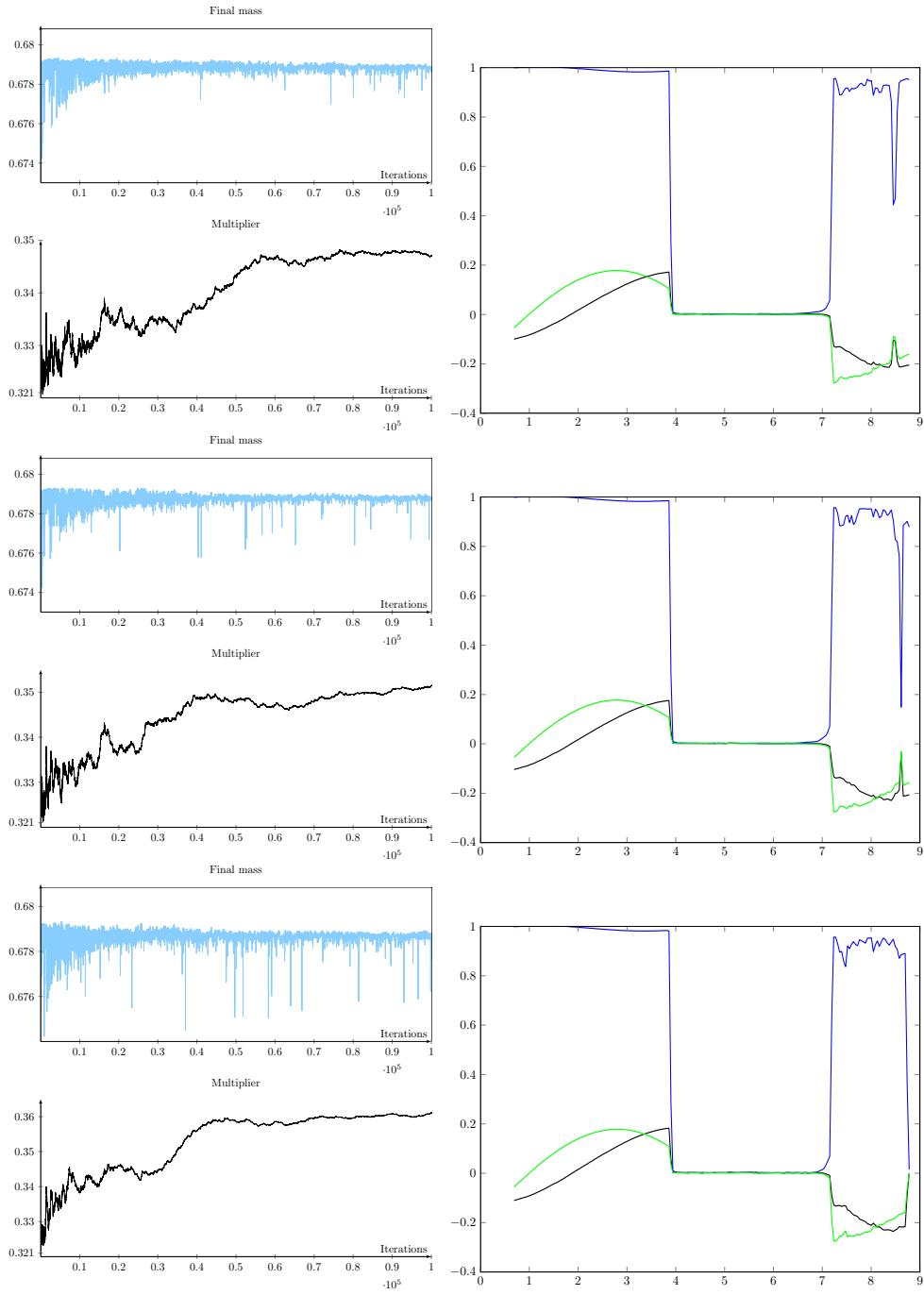


Figure 4: Results for  $p = 0.980$  (top),  $p = 0.985$  (middle) and  $p = 0.990$  (bottom)

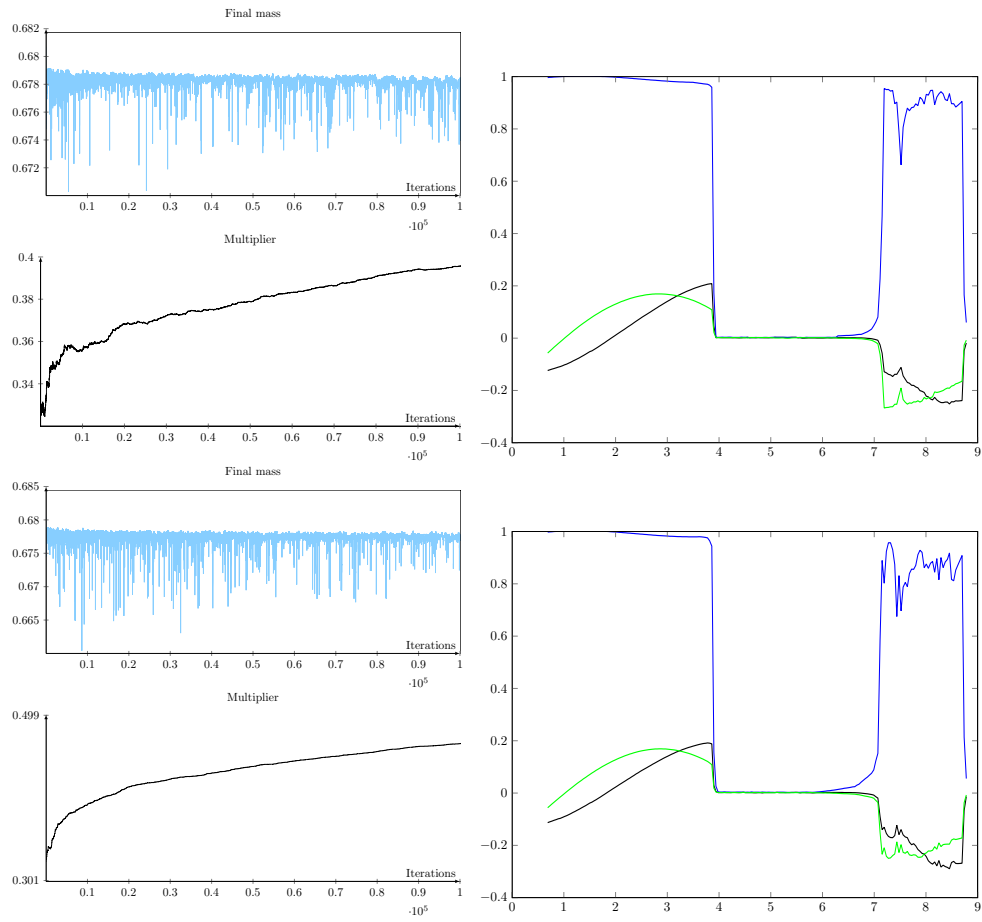


Figure 5: Results for  $p = 0.995$  (top) and  $p = 0.999$  (bottom)

optimal consumption of the no-failure trajectory on the other hand (each point on these curves corresponds to a run of the stochastic Arrow-Hurwicz algorithm).

The first curve (Figure 6) illustrates the consistency of the results obtained. We can see that the multiplier (which corresponds to the sensitivity of the optimal cost to the probability level  $p$ ) increases with  $p$ , with a break in the slope at a probability level of around 0.960.

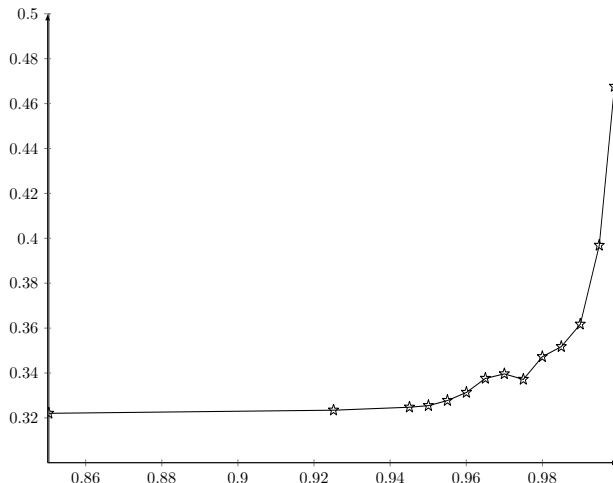


Figure 6: Multiplier  $\mu$  as a function of the probability level  $p$

The second curve (Figure 7) has a more direct interpretation, since it indicates the amount of fuel needed to reach the end of the no-failure scenario, according to the requested level of probability of success of the mission. Once again, we see a break at around  $p = 0.960$ , as consumption starts to increase much more rapidly after this value. We can therefore deduce that there is a probability threshold above which security “comes at a high price”. Note that the fuel consumption for the no-failure scenario shown in Figure 7 does not correspond to the amount of fuel you would need to carry to complete the mission with a given level of probability. Indeed, this amount of fuel doesn’t take into account the recourse control consumption, which could be numerically estimated by Monte Carlo approach. This calculation was not carried out in this study.

## 6 Conclusions and perspectives

In this study dedicated to the design of “robust” interplanetary trajectories, we believe that we have shown that the method that consists in solving the problem of minimizing fuel consumption in expectation under the probability constraint of reaching the final target by the stochastic gradient method works effectively. This involved overcoming a number of difficulties, such as choosing a suitable problem parametrization, dealing with the final target constraint of the no-failure scenario by projection, among others. The results are sufficiently clear, at least for probability levels  $p$  up to 0.990, to highlight the modifications of the optimal control as a function of  $p$ . Moreover, the convergence of the stochastic algorithm, although slow (but this is largely due to the way in which the coefficient for smoothing the constraint in probability must decrease), is reasonable in the majority of cases studied. However, much remains to be done, both theoretically and numerically.

- As far as theory is concerned, and as suggested in Appendices C and D, we need to understand how the inner problem can be formulated with the Heaviside function  $Y$  (for which a theory of smoothing exists: see [2]). This question is all the more important in practical terms as the smoothing of the function  $Y$  can be performed symmetrically with respect to the point of discontinuity, and this leads

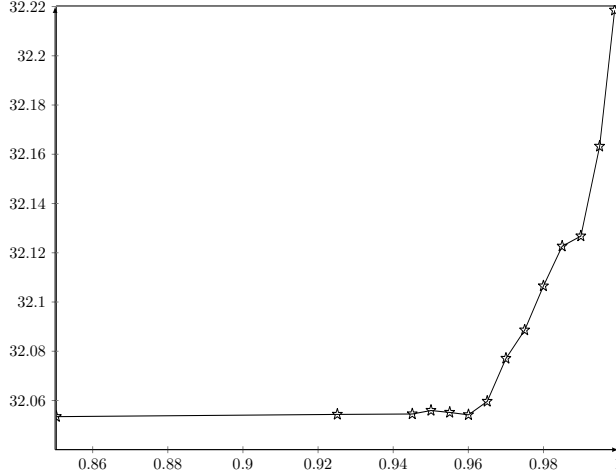


Figure 7: Fuel consumption (multiplied by  $10^2$ ) as a function of the probability level  $p$

to an optimal rule of decreasing smoothing coefficient in  $k^{-1/5}$  and decreasing mean square error in  $k^{-4/5}$  (division by 10,000 in 100,000 iterations). In the case of non-symmetrical smoothing, we move to an optimal rule in  $k^{-1/3}$  and a mean-square error decreasing in  $k^{-2/3}$  (division by about 2,000 in 100,000 iterations). By Appendix C, we are convinced that direct smoothing of  $I$  is equivalent to a non-symmetrical smoothing of  $Y$ , that is, not the best rule to decrease the mean square error.

- From the numerical point of view, the overall calculation time is enormous, making the operational use of the program still too cumbersome. Part of the explanation lies in the number of iterations required, as explained above. The other part of the explanation comes from the cost of solving a single iteration, which requires the complete resolution of two deterministic optimal control problems. Any progress on either of these two operations, and particularly the first, would have a beneficial effect on this overall computation time.

## A Satellite model details

### A.1 Change of coordinates

We recall here the simplified dynamic model of a satellite given in Equation 1

$$\frac{dr}{dt} = v, \quad \frac{dv}{dt} = -\nu \frac{r}{\|r\|^3} + \frac{T}{m} \kappa, \quad \frac{dm}{dt} = -\frac{T}{g_0 I_{sp}} \delta,$$

and rewrite this state dynamics using the equinoctial coordinates  $(p, e_x, e_y, h_x, h_y, l)$ , for the position and velocity of the satellite. The equinoctial coordinates are obtained from the Keplerian coordinates<sup>10</sup>  $(a, e, i, \omega, \Omega, \nu)$

<sup>10</sup>semi-major axis, eccentricity, inclination, argument of periapsis, longitude of the ascending node, and true anomaly

through the transformation:

$$\begin{aligned}
p &= a|1 - e^2| , \\
e_x &= e \cos(\omega + \Omega) , \\
e_y &= e \sin(\omega + \Omega) , \\
h_x &= \tan(i/2) \cos(\Omega) , \\
h_y &= \tan(i/2) \sin(\Omega) , \\
l &= \omega + \Omega + \nu ,
\end{aligned}$$

and by performing the following change of variables for the control inputs:<sup>11</sup>

$$\begin{aligned}
q &= \delta \cos(\beta) \cos(\alpha) , \\
s &= \delta \cos(\beta) \sin(\alpha) , \\
w &= \delta \sin(\beta) ,
\end{aligned}$$

where  $q$ ,  $s$  and  $w$  are the radial, tangential, and normal components of the control input, respectively. In this coordinate system, Gauss' equations are written as:

$$\frac{dp}{dt} = 2 \sqrt{\frac{p^3}{\nu}} \frac{1}{Z} \frac{T}{m} s , \quad (29a)$$

$$\frac{de_x}{dt} = \sqrt{\frac{p}{\nu}} \frac{1}{Z} \frac{T}{m} (Z \sin(l) q + A s - e_y F w) , \quad (29b)$$

$$\frac{de_y}{dt} = \sqrt{\frac{p}{\nu}} \frac{1}{Z} \frac{T}{m} (-Z \cos(l) q + B s + e_x F w) , \quad (29c)$$

$$\frac{dh_x}{dt} = \frac{1}{2} \sqrt{\frac{p}{\nu}} \frac{X}{Z} \cos(l) \frac{T}{m} w , \quad (29d)$$

$$\frac{dh_y}{dt} = \frac{1}{2} \sqrt{\frac{p}{\nu}} \frac{X}{Z} \sin(l) \frac{T}{m} w , \quad (29e)$$

$$\frac{dl}{dt} = \sqrt{\frac{\nu}{p^3}} Z^2 + \sqrt{\frac{p}{\nu}} \frac{1}{Z} F \frac{T}{m} w , \quad (29f)$$

$$\frac{dm}{dt} = -\frac{T}{g_0 I_{sp}} \sqrt{q^2 + s^2 + w^2} , \quad (29g)$$

with :

$$\begin{aligned}
Z &= 1 + e_x \cos(l) + e_y \sin(l) , \\
A &= e_x + (1 + Z) \cos(l) , \\
B &= e_y + (1 + Z) \sin(l) , \\
F &= h_x \sin(l) - h_y \cos(l) , \\
X &= 1 + h_x^2 + h_y^2 .
\end{aligned}$$

To apply variational techniques, we assume that the engine on/off indicator can vary continuously between the values 0 (off) and 1 (on), so that the constraint on the control input is written as:

$$q^2 + s^2 + w^2 \leq 1 . \quad (30)$$

---

<sup>11</sup>where  $\alpha$  is the azimuth measured relative to  $q$  and  $\beta$ , the elevation of the engine thrust in the satellite's local frame of reference

Finally, the initial time  $t_i$  is assumed to be fixed, and the state at the initial time is assumed to be known giving  $x(t_i) = x_i$ . Thus, with  $x = (p, e_x, e_y, h_x, h_y, l)^\top$  and  $u = (q, s, w)^\top$ , the equinoctial state dynamics (29) can be summarized as

$$x(t_i) = x_i, \quad \frac{dx}{dt}(t) = f(x(t), u(t)), \quad (31)$$

which gives Equation (2b).

## A.2 Deterministic optimization problem

We recall that the final time  $t_f$  is also fixed. The optimization problem we aim to solve consists of enforcing a rendez-vous constraint in position/velocity (which thus affects the first six components of the state), with the objective of maximizing the mass at the final time  $t_f$ .

Let  $\lambda = (\lambda_p, \lambda_{e_x}, \lambda_{e_y}, \lambda_{h_x}, \lambda_{h_y}, \lambda_l, \lambda_m)^\top$  be the adjoint state associated with the dynamics (29), the Hamiltonian of the problem is expressed as (with no integral term in the cost):

$$H(x, u, \lambda) = \lambda^\top f(x, u), \quad (32)$$

The dynamics of the adjoint state  $\lambda$  are given by:<sup>12</sup>

$$\frac{d\lambda}{dt} = -\left(\frac{\partial f}{\partial x}(x, u)\right)^\top \lambda. \quad (33)$$

The gradients of the Hamiltonian with respect to the control inputs are written as:

$$\left(\frac{\partial f}{\partial u}(x, u)\right)^\top \lambda, \quad (34)$$

with :

$$\frac{\partial f}{\partial u}(x, u) = \begin{pmatrix} 0 & 2K_a p & 0 \\ K_a Z \sin(l) & K_a A & -K_a e_y F \\ -K_a Z \cos(l) & K_a B & K_a e_x F \\ 0 & 0 & \frac{1}{2} K_a X \cos(l) \\ 0 & 0 & \frac{1}{2} K_a X \sin(l) \\ 0 & 0 & K_a F \\ \gamma q_n & \gamma s_n & \gamma w_n \end{pmatrix},$$

where  $q_n$ ,  $s_n$  and  $w_n$  are the normalized control inputs, that is  $q_n = \frac{q}{\sqrt{q^2 + s^2 + w^2}}$ ,  $\dots$ , and where the two variables  $\gamma$  and  $K_a$  are defined as:

$$\gamma = -\frac{T}{g_0 I_{sp}},$$

$$K_a = \sqrt{\frac{p}{\nu} \frac{T}{m} \frac{1}{Z}}.$$

The final cost to minimize consists, on one hand, of the term corresponding to the negative of the mass at the final time, and on the other hand, of a term corresponding to the dualization of the final target constraints<sup>13</sup> using an augmented Lagrangian with a regularization parameter  $c$ , the multiplier being denoted as  $\mu^d$ , thus in total:

$$x_7(t_i) - x_7(t_f) + \sum_{j=1}^6 \mu_j^d (x_j(t_f) - x_{f,j}) + \frac{c}{2} (x_j(t_f) - x_{f,j})^2. \quad (35)$$

<sup>12</sup>The explicit form of these equations is relatively complicated, and therefore it will not be provided in this note. The reader is referred to [12] for the complete expression

<sup>13</sup>Recall that our goal is to use a stochastic algorithm to solve the optimization problem under probabilistic constraints. Therefore, we are compelled to dualize the final target constraints

The transversality conditions then provide the value of the adjoint state at the final time:

$$\lambda(t_f) = \begin{pmatrix} \mu_1^d + c(x_1(t_f) - x_{f,1}) \\ \mu_2^d + c(x_2(t_f) - x_{f,2}) \\ \mu_3^d + c(x_3(t_f) - x_{f,3}) \\ \mu_4^d + c(x_4(t_f) - x_{f,4}) \\ \mu_5^d + c(x_5(t_f) - x_{f,5}) \\ \mu_6^d + c(x_6(t_f) - x_{f,6}) \\ -1 \end{pmatrix}. \quad (36)$$

The deterministic optimization problem is solved by the deterministic Arrow-Hurwicz algorithm. An iteration of this algorithm consists of:

- Integrating the state dynamics (29) over the interval  $[t_i, t_f]$  using the current control input  $u$ .
- Integrating the adjoint state dynamics (33) from the conditions (36) backward in time.
- Updating the control input trajectories  $u$  using the gradients (34), with projection onto the set defined by (30).
- Performing a gradient step on the dual variables  $(\mu_1^d, \dots, \mu_6^d)$ .

## B Transformation lemma

Consider the following optimization problem:

$$\min_{\mathbf{u} \in U^{\text{ad}} \subset \mathcal{U}} \frac{J(\mathbf{u})}{\Theta(\mathbf{u})} \quad \text{s.t.} \quad \Theta(\mathbf{u}) \geq p, \quad (37)$$

in which  $J$  and  $\Theta$  assume positive values. Problem (37) displays a very special structure, in the sense that the denominator in the ratio defining the cost function is identical to the left-hand side of the constraint.

The following lemma provides conditions under which Problem (37) and the optimization problem

$$\min_{\mathbf{u} \in U^{\text{ad}} \subset \mathcal{U}} J(\mathbf{u}) \quad \text{s.t.} \quad \Theta(\mathbf{u}) \geq p, \quad (38)$$

have the same solutions.

**Lemma 5** *Let  $U^{\text{ad}}$  be a closed convex subset of the Hilbert space  $\mathcal{U}$ . Let  $J$  and  $\Theta$  be real-valued differentiable functions defined on  $\mathcal{U}$ . We moreover assume that  $J$  is nonnegative and that  $\Theta$  is positive.*

- Let  $\mathbf{u}^*$  be a solution of (37). If  $\mathbf{u}^*$  satisfies the condition

$$\Theta(\mathbf{u}^*) = p,$$

then  $\mathbf{u}^*$  is also a solution of (38).

- Conversely, suppose that  $\mathbf{u}^*$  satisfies the Karush-Kuhn-Tucker conditions of Problem (38), and let  $\mu^*$  be the associated multiplier. If  $\mu^*$  is such that

$$\mu^* \geq \frac{J(\mathbf{u}^*)}{\Theta(\mathbf{u}^*)},$$

then  $\mathbf{u}^*$  also satisfies the Karush-Kuhn-Tucker conditions of Problem (37).

**Proof.** Assume that  $\mathbf{u}^*$  is a solution of (37) such that  $\Theta(\mathbf{u}^*) = p$ . Then

$$\frac{J(\mathbf{u}^*)}{\Theta(\mathbf{u}^*)} \leq \frac{J(\mathbf{u})}{\Theta(\mathbf{u})} \quad \forall \mathbf{u} \in U^{\text{ad}} \cap \{\mathbf{u} \in \mathcal{U}, \Theta(\mathbf{u}) \geq p\}.$$

The left-hand side of the last inequality is equal to  $J(\mathbf{u}^*)/p$ , whereas the right-hand side is less than or equal to  $J(\mathbf{u})/p$ . Hence  $\mathbf{u}^*$  is a solution of Problem (38).

Conversely, let  $(\mathbf{u}^*, \mu^*)$  be a pair satisfying the Karush-Kuhn-Tucker conditions of (38):<sup>14</sup>

$$\begin{aligned} \nabla J(\mathbf{u}^*) - \mu^* \nabla \Theta(\mathbf{u}^*) &\in -N_{U^{\text{ad}}}(\mathbf{u}^*), \\ \mu^* &\geq 0, \quad \Theta(\mathbf{u}^*) \geq p, \quad \mu^*(\Theta(\mathbf{u}^*) - p) = 0, \end{aligned}$$

where  $N_{U^{\text{ad}}}(\mathbf{u}^*)$  is the normal cone to  $U^{\text{ad}}$  at  $\mathbf{u}^*$ . Let  $\lambda^*$  be defined by:

$$\mu^* = \frac{J(\mathbf{u}^*)}{\Theta(\mathbf{u}^*)} + \lambda^* \Theta(\mathbf{u}^*).$$

From the assumptions on  $\mu^*$  and  $\Theta$ , we deduce that  $\lambda^* \geq 0$ . Moreover, the condition  $\mu^*(\Theta(\mathbf{u}^*) - p) = 0$  implies:

$$\frac{J(\mathbf{u}^*)}{\Theta(\mathbf{u}^*)} (\Theta(\mathbf{u}^*) - p) + \lambda^* \Theta(\mathbf{u}^*) (\Theta(\mathbf{u}^*) - p) = 0,$$

and thus  $\lambda^*(\Theta(\mathbf{u}^*) - p) = 0$  because both terms in the last expression are nonnegative. Finally, substituting  $\mu^*$  by its expression function of  $\lambda^*$  in the first Karush-Kuhn-Tucker condition of Problem (38) leads to:

$$\nabla J(\mathbf{u}^*) - \frac{J(\mathbf{u}^*)}{\Theta(\mathbf{u}^*)} \nabla \Theta(\mathbf{u}^*) - \lambda^* \Theta(\mathbf{u}^*) \nabla \Theta(\mathbf{u}^*) \in -N_{U^{\text{ad}}}(\mathbf{u}^*).$$

We thus conclude that  $(\mathbf{u}^*, \lambda^*)$  satisfies the Karush-Kuhn-Tucker conditions of Problem (37).  $\square$

## C Choosing the smoothing parameter $r_k$

In [2] and [1], a general problem of minimizing a criterion in expectation under a probability constraint is studied. This probability constraint, as in our study, is written as a constraint in expectation involving the (discontinuous) Heaviside function  $Y$ :

$$Y(y) = \begin{cases} 0 & \text{if } y < 0, \\ 1 & \text{otherwise.} \end{cases}$$

In order to numerically deal with this constraint in expectation, the function  $Y$  is regularized by convolution (see [13]) with a smoothing parameter  $r$ . If the regularized function  $Y_r$  is chosen symmetrical ( $Y_r(-x) = Y_r(x)$ ), it is shown in [2, Theorem 3] that minimizing the mean square error of the estimate of the derivative of the smoothed constraint leads to a parameter  $r$  proportional to  $k^{-1/5}$  when the estimation is based on  $k$  samples. Choosing a non symmetrical regularized function  $Y_r$  such as

$$Y_r(y) = \begin{cases} 0 & \text{if } y \leq -r, \\ 1 + \frac{y}{r} & \text{if } y \in ]-r, 0[, \\ 1 & \text{otherwise,} \end{cases} \quad (39)$$

is possible and leads to choose a smoothing parameter  $r$  proportional to  $k^{-1/3}$ .

<sup>14</sup>We assume here that some constraint qualification condition holds, so that these conditions are necessary optimality conditions for Problem (38).

In our study, the function involved in the expected constraint is the indicator function  $I$  as defined in Equation (7), instead of the Heaviside function  $Y$  in [2]. As given in Equation (14), the indicator function  $I$  is regularized as

$$I_r(y) = \max \left\{ 0, 1 - \frac{y}{r} \right\}, \quad y \geq 0. \quad (40)$$

The regularized indicator function  $I_r$  enters the inner optimization Problem (20). We show that this regularized problem involving function  $I_r$  in (40) is equivalent to an other optimization problem involving function  $Y_r$  in (39). For that purpose, consider a failure  $\xi = (t_p, t_d)$  and the satellite state  $x(t_p)$  at the beginning of the failure. We define  $G$  as a mapping which is non-negative when reaching the target after the failure is possible and negative otherwise. Thus, the space is divided into two parts according to the sign of the function  $G$ , the first part corresponding to the points from which the target can be reached. Now, the condition  $C(x^\xi(t_f^\xi)) = 0$  is equivalent to the condition  $G(x(t_p), t_p, t_d) \geq 0$ , that is,

$$I\left(\|C(x^\xi(t_f^\xi))\|\right) = Y\left(G(x(t_p), t_p, t_d)\right), \quad (41)$$

and therefore, the analog of the smoothing function (40) of  $I$  for function  $Y$  is (39). As already discussed, the non symmetrical smoothing  $Y_r$  leads to a smoothing coefficient  $r_k$  proportional to  $k^{-1/3}$ . Thus, we also choose a smoothing coefficient  $r_k$  proportional to  $k^{-1/3}$  for  $I_r$ .

## D Remarks on the inner problem and its gradients

Here again, we use the function  $G$  introduced in Appendix C. Using (41), the inner optimization problem (20) becomes:

$$W_r(x(t_p), t_p, t_d, \mu) = \min_v \left( K(\Psi_{t_i, t_f}^{(u, \mathbf{V}, \mathbf{T}_p, \mathbf{T}_d)}(x_i)) - \mu \right) Y_r\left(G(x(t_p), t_p, t_d)\right). \quad (42)$$

We are interested in the value and in the different partial derivatives of  $W_r$  (with respect the control  $v$ , to the initial state  $x$  and to the multiplier  $\mu$ ) as they appear in the stochastic Arrow-Hurwicz algorithm in §4.2. There are several cases to consider.

1.  $Y_r(G(x(t_p), t_p, t_d)) = 0$ , that is, we miss the target by at least  $r$ : then  $Y_r$  and its gradient are equal to zero, and so are  $W_r(x(t_p), t_p, t_d, \mu)$  and its partial derivatives.
2.  $Y_r(G(x(t_p), t_p, t_d)) = 1 + \theta/r$ , that is, we approach the target at less than  $r$ : then the partial derivatives are of order  $1/r$  since the derivative of  $Y_r$  is of order  $1/r$ .
3.  $Y_r(G(x(t_p), t_p, t_d)) = 1$ , that is, we hit the target exactly: then the gradient of  $Y_r$  is equal to zero, so that the partial derivatives of  $W_r$  only come from the final cost  $K$  and do not depend on  $r$ .

As a consequence, when one is at a distance less than  $r$  from the target without being exactly there, the gradient of  $Y_r$  with respect to the control is of order  $1/r$ , so that the inner optimization problem will try of getting as close possible of the target.

Another conclusion is that, in order to properly evaluate the gradients of the function  $W_r$  with respect to the state  $x$  and the multiplier  $\mu$  as required in the stochastic Arrow-Hurwicz algorithm in §4.2, it is necessary to distinguish the case when the target is hit exactly from the case where the target is approached at less than  $r$ .

## References

- [1] L. Andrieu, G. Cohen, and F. J. Vazquez-Abad. Stochastic programming with probability constraints. *arXiv preprint*, arXiv:0708.0281, 2007.
- [2] L. Andrieu, G. Cohen, and F. J. Vazquez-Abad. Gradient-based simulation optimization under probability constraints. *European Journal of Operational Research*, 212(2):345–351, 2011.

- [3] K. J. Arrow, L. Hurwicz, H. Uzawa, H. B. Chenery, S. Johnson, and S. Karlin. *Studies in linear and non-linear programming*, volume 2. Stanford University Press, 1958.
- [4] D. Bertsimas, D. B. Brown, and C. Caramanis. Theory and applications of robust optimization. *SIAM Review*, 53:464–501, 2011.
- [5] J. F. Bonnans. The shooting approach to optimal control problems. *IFAC Proceedings Volumes*, 46(11):281–292, 2013.
- [6] P. Carpentier and G. Cohen. *Decomposition-coordination en optimisation déterministe et stochastique*, volume 81 of *Mathématiques et Applications*. Springer, 2017.
- [7] R. Chai, A. Savvaris, A. Tsourdos, S. Chai, and Y. Xia. A review of optimization techniques in spacecraft flight trajectory design. *Progress in aerospace sciences*, 109:100543, 2019.
- [8] B. A. Conway. *Spacecraft trajectory optimization*, volume 29. Cambridge University Press, 2010.
- [9] J. C. Culioli and G. Cohen. Decomposition/coordination algorithms in stochastic optimization. *SIAM Journal on Control and Optimization*, 28(6):1372–1403, 1990.
- [10] J.-C. Culioli and G. Cohen. Optimisation stochastique sous contraintes en esperance. Technical Report A-288, Rapport interne CAS, ENSMP, December 1994.
- [11] J.-C. Culioli and G. Cohen. Optimisation stochastique sous contraintes en esperance. *Comptes Rendus de l’Académie des Sciences*, 320(I):735–758, 1995.
- [12] T. Dargent. Transfert d’orbite optimal par application du principe du minimum. Logiciel T3D, version 2, 2004.
- [13] Y. Ermoliev, V. Norkin, and R.-B. Wets. The minimization of semicontinuous functions: Mollifier subgradients. *SIAM Journal on Control and Optimization*, 33(1):149–167, 1995.
- [14] C. Greco, S. Campagnola, and M. Vasile. Robust space trajectory design using belief optimal control. *Journal of Guidance, Control and Dynamics*, 45(6):1060–1077, 2022.
- [15] R. Henrion. On the connectedness of probabilistic constraint sets. *Journal of Optimization Theory and Applications*, 112:657–663, 2002.
- [16] R. Henrion and W. Romisch. Holder and lipschitz stability of solution sets in programs with probabilistic constraints. *Mathematical Programming*, 100:589–611, 2004.
- [17] R. Henrion and C. Strugarek. Convexity of chance constraints with independent random variables. *Computational Optimization and Applications*, 41(2):263–276, 2008.
- [18] D. Morante, M. Sanjurjo Rivo, and M. Soler. A survey on low-thrust trajectory optimization approaches. *Aerospace*, 8(3):88, 2021.
- [19] K. Oguri and G. Lantoine. Stochastic sequential convex programming for robust low-thrust trajectory design under uncertainty. In *AAS/AIAA Astrodynamics Specialist Conference*, volume 8. AAS Charlotte, NC, 2022.
- [20] J. T. Olympio. Designing robust low-thrust interplanetary trajectories subject to one temporary engine failure. In *Proceedings of the 20th AAS/AIAA Space Flight Meeting*, pages 10–171, 2010.
- [21] A. Prekopa. *Stochastic Programming*. Kluwer Academic Publishers, Dordrecht, 1995.
- [22] A. Prekopa. Probabilistic programming. In *Stochastic Programming*, volume 10 of *Handbooks in Operations Research and Management Science*, pages 267–351. Elsevier, 2003.

- [23] R. T. Rockafellar and R. J.-B. Wets. *Variational Analysis*. Springer Verlag, Berlin Heidelberg, 1998.
- [24] A. Rubinsztein, C. G. Sandel, R. Sood, and F. E. Laipert. Designing trajectories resilient to missed thrust events using expected thrust fraction. *Aerospace Science and Technology*, 115:106780, 2021.
- [25] A. Ruszczyński and A. Shapiro. *Handbook in Operations Research and Management Science, Vol. 10 - Stochastic Programming*. Elsevier, 2003.
- [26] A. Shapiro, D. Dentcheva, and A. Ruszczyński. *Lectures on Stochastic Programming: Modeling and Theory*. SIAM and MPS, Philadelphia, second edition, 2014.
- [27] Y. Shimane and K. Ho. Robustness assessment of low-thrust trajectory via sequentially truncated sim-flanagan problems. In *ASCEND 2021*, page 4153. American Institute of Aeronautics and Astronautics, 2021.
- [28] A. Shirazi, J. Ceberio, and J. A. Lozano. Spacecraft trajectory optimization: A review of models, objectives, approaches and solutions. *Progress in Aerospace Sciences*, 102:76–98, 2018.
- [29] Y. Sidhoum and K. Oguri. Robust low-thrust trajectory correction planning under uncertainty: Primer vector theory approach. In *AAS/AIAA Astrodynamics Specialist Conference, Broomfield, CO, USA*, 2024.
- [30] C. Venigalla, J. A. Englander, and D. J. Scheeres. Multi-objective low-thrust trajectory optimization with robustness to missed thrust events. *Journal of Guidance, Control and Dynamics*, 45(7):1255–1268, 2022.
- [31] A. Zavoli and L. Federici. Reinforcement learning for robust trajectory design of interplanetary missions. *Journal of Guidance, Control and Dynamics*, 44(8):1440–1453, 2021.